Journal of Inorganic Biochemistry 192 (2019) 126–139

Contents lists available at ScienceDirect

Journal of Inorganic Biochemistry

journal homepage: www.elsevier.com/locate/jinorgbio

Dinuclear copper(II) complexes of "end-off" bicompartmental ligands: Alteration of the chelating arms on ligands to regulate the reactivity of the complexes towards DNA

Shuhong Cao[a,1], Run Cheng[b,1], Dandan Wang[a], Yunfeng Zhao[a], Ruiren Tang[b], Xiuli Yang[a,*], Jingwen Chen[a,*]

[a] School of Chemistry and Chemical Engineering, Building Materials Research Academy, Yancheng Institute of Technology, Jianjun East Rd. 211, Yancheng 224051, PR China

[b] School of Chemistry and Chemical Engineering, Central South University, Changsha 410000, PR China

ARTICLE INFO

Keywords:
Artificial nuclease
Dinuclear copper(II) complex
DNA cleavage
Ligand modification
Substituent effect

ABSTRACT

Two phenol-based "end-off" biscompartmental heptadentate ligands were designed by introduction of substituents with different electronic and steric properties to the chelating arms, *i.e.* 2,6-bis{[(2-pyridylmethyl)(2-hydroxyethyl)amino]methyl}-4-methylphenol (**L**^{1}) and 2,6-bis{[(2-aminoethyl)(2-hydroxyethyl)amino]methyl}-4-methylphenol (**L**^{2}). The dinuclear copper(II) complexes (**1** and **2**) of the ligands were synthesized and evaluated as potential nuclease models. The basicity behavior and coordination property of each ligand towards Cu(II) ion in aqueous solution were investigated by pH potentiometric titrations accompanied by ESI-MS and spectrometry. Both ligands show a strong tendency to chelate Cu(II) generating dinuclear copper(II) complexes in Cu(II)/**L** molar ratio of 2:1 in the pH range of 3–11, and when pH is 7.40 the cationic OH^--bridged dicopper (II) complexes were determined to be the dominant species. Studies on the interactions of **1** and **2** with Calf Thymus DNA relevant to DNA binding exhibit a pronounced impact of the substituents tethered on the chelating arms of the ligands. Assessment by agarose gelelectrophoresis of the plasmid pBR322 DNA cleavage activity in the presence of Vc under aerobic conditions evidence significant cleavage efficiency of the two complexes, displaying a reactivity order of **1** < **2**. The mechanistic studies suggest that the cleavage implements *via* an oxidative pathway, where hydroxyl radical and hydrogen peroxide are responsible for the cleavage reactions. For **2**, additional singlet oxygen seems to be involved in the cleavage. The differences between the two complexes in DNA binding and cleavage were discussed in relation to the electronic and steric properties of the substituents on the chelating arms imposed by each phenoxido ligand.

1. Introduction

Polynuclear metal complexes derived from multidentate ligands have attracted extensive interests from the scientific communities for their interesting structures and occasionally novel properties [1,2]. Many polynuclear complexes have been used as potential models for the metallobiosites essential for catalytic activity found in a number of natural metalloenzymes [3–5]. Superior to mononuclear architectures, polynuclear ones in most cases facilitate the cooperation between metal centers in close proximity as found in many metalloenzmyes, which was proven critical in improving their reactivities [6]. The dinuclear complexes derived from compartmental dinucleating ligands have received particular interests, and quite a number of metalloenzmye mimics reported so far are based on such type of ligands [1,7–18]. Of the dinucleating ligands reported, the phenol-based "end-off" compartmental ligands, which possess two or four symmetrical or asymmetrical pendent chelating arms attached to the 2- and 6-position of the central phenol ring, attracted intense attentions due to their rich coordination chemistry with a wide variety of metal ions. They can usually accommodate two metal ions into adjacent coordination chambers producing endogenously phenoxido-bridged homo- or hetero-dinuclear complexes under controlled reaction conditions [1,7–10,12,14–19]. In some cases, ancillary functionalities such as hydroxido, methoxide, azido, carboxylato, halido, *etc.* may be present in the complexes [7–10,20]. The specific typology of such ligands facilitates the two metal ions in a close proximity in a single molecular entity for their cooperativity in

* Corresponding authors.
E-mail addresses: xlyang@ycit.edu.cn (X. Yang), jwchen@ycit.edu.cn (J. Chen).
[1] These authors contributed equally to this work.

https://doi.org/10.1016/j.jinorgbio.2018.12.014
Received 23 July 2018; Received in revised form 23 December 2018; Accepted 24 December 2018
Available online 30 December 2018
0162-0134/

enhancing catalysis, making the resultant complexes the preferred candidates as metalloenzyme mimics [3,6]. A plenty of dinuclear complexes of such ligands have been constructed and widely used in mimicking the bimetallic active sites in metalloenzymes, with the aim to gain insights into the structural and/or functional aspects of the biological catalysts, and to elucidate their catalytic mechanism as well as the plausible catalytic roles of the metal ions in the biological molecules [7,8,10,12–14,16–18,21]. What intrigues us most is that many of these complexes demonstrated different extent of ability to reproduce the structural and/or functional characteristics of metallonuclease [8,10,12,13,15–18,22,23]. Actually, the preparation of metal complexes as chemical nucleases have received ongoing attention [6,18,24–32] since the well-known $[Cu(Phen)_2]^{2+}$ (Phen = 1, 10-phenanthroline) complex was proved to be an effective chemical nuclease [33], and found to be useful in nucleic acid and protein studies [34] and as an important template for design of cytotoxic metallodrugs [35,36]. A number of these complexes displayed potential applications in fields of molecular biological technology [30] and pharmaceutical development [32].

Ligands are known to play a crucial role in tuning structure, physico-chemical properties, and therefore reactivities of the generated complexes. Numerous studies have revealed the effects of modifications of a ligand molecule on the catalytic activities of the resultant complexes as metalloenzyme mimics [11,15,37–51]. In nature, many nucleases was found to employ cooperation of amino acid side chains with metal-ion cofactors present in the active sites to catalyze the cleavage of phosphate esters [25]. Enlightened by this finding, efforts have been made to follow this feature through attachment of auxiliary functional groups such as hydrogen-bond substituents, *e.g.* amino, ammonium, or guanidine groups [6,11,15,39,42–49], to the metal chelating ligand. In most cases, the resulting complexes achieve effective catalysis in phosphate ester cleavage relative to the unfunctionalized counterparts. For examples, a copper(II) complex of a bipyridine ligand tethering two ammonium arms pioneered by Krämer and Kövári [43] indicated a great increase in the hydrolysis rate of bis(*p*-nitrophenyl)phosphate (BNPP) compared with the control structure missing ammonium ions. A series of polypyridine-based metal complexes functionalized by amino hydrogen bond donors on the pyridyl units of the ligands designed by groups of Williams [11], Chin [39,45,46] and Mareque-Rivas [47], et al. also showed more effective in promoting the cleavage of DNA- and RNA-like models than the homologous complexes without amino groups. Some even yielded a comparable catalytic efficacy to the introduction of a second metal ion for enhancing its activity. A similar observation was reported by Xu et al. [48] using a 1,7-dioxa-4,10-diazacyclododecane-based mononuclear copper(II) complex bearing two ethylamino or ethylguanidino side arms to cleave plasmid pUC19 supercoiled DNA. Amino alcohol functional groups are also often found in biologically active molecules [52] and ligands [18,27,50,51,53]. The related studies demonstrated that the introduction of alkanol pendants to the chelating units of a ligand likewise showed an efficient modification for enhancing the binding and catalytic activity of the functionalized complexes towards phosphate esters or other substrates [42]. The presence of alkylhydroxyl groups in a copper(II) complex appears to potentially increase affinity of the complex to DNA, and plays a critical role in DNA cleavage [50,51].

The phenol-based compartmental compounds have been shown to possess diverse coordination properties, and their derivatives provide excellent possibilities for the design of tailored chelating agents which exert influence on the structure, stability, or electronic properties, and catalysis of the metal complexes [37,38]. A lot of elegant researches

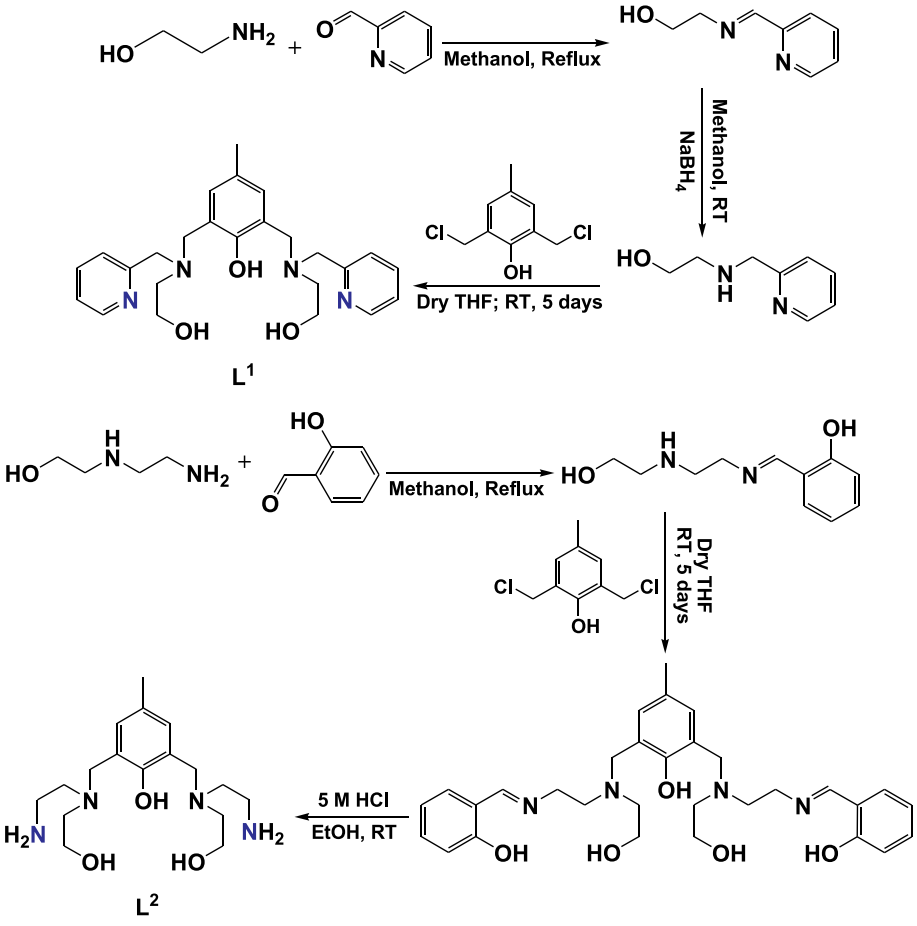

Scheme 1. Synthetic procedures of ligands L^1 and L^2.

have been conducted on the effects of introduction of different electron donating-withdrawing substituents to the central phenol ring of this type of ligands on the reactivities of the resultant complexes [24,37,38,41,54]. Further studies of the role of the substituents present on the periphery of the backbone of the ligands in affecting the properties of the complexes, both from an experimental and theoretical point of view, are still being pursued. Our laboratory is engaged in exploring the structure-reactivity relationship of multinuclear metal complexes as mimics of biosites in metallonucleases [55,56]. In continuation to our efforts, we herein design two dicopper(II) complexes (**1** and **2**) of acyclic phenol-based bicompartmental ligands, 2,6-bis{[(2-pyridylmethyl)(2-hydroxyethyl)amino]methyl}-4-methylphenol ($\mathbf{L^1}$) and 2,6-bis{[(2-aminoethyl)(2-hydroxyethyl)amino] methyl}-4-methylphenol ($\mathbf{L^2}$) (Scheme 1). $\mathbf{L^1}$ and $\mathbf{L^2}$ are homologous ditopic N_4O_3-coordinating heptadentate ligands having two mixed chelating pendants linked at 2, 6-position of the central phenol moiety through an articular tertiary nitrogen atom. Each ligand features two flexible ethylhydroxyl side arms whereas differs in the other chelating arms offering distinct N donors, *i.e.* two aromatic pyridyl-N and two alkylamino-N donors, respectively. The two complexes **1** and **2** were evaluated as metallonuclease functional models to investigate the possible impacts of the modifications of the pendent chelating arms of the ligands on the DNA binding ability and cleaving reactivity of the complexes. It is expected that the alteration of the donor type and basicity, the steric and electronic properties as well as the rigidity-flexiblity of the chelating arms may affect the Cu(II) complexation, the stability and geometric/structural property of the resultant complexes, and therefore may exert profound influence on their DNA binding ability and cleavage activity.

2. Experimental

2.1. Materials and techniques

All chemicals obtained commercially are of reagent grade or analytical grade, and used without further purification if not stated otherwise. Solvents used in this work were purified by the reported procedures [57] prior to use. Deuterated compounds D_2O, DMSO-d_6 and chloroform-d_1 were obtained from Cambridge Isotope Laboratories. The reagents for synthesis of the two ligands, *p*-cresol, 2-(2-aminoethylamino)ethanol, ethanolamine, 2-aminoethanol, picolinaldehyde, salicylaldehyde and trimethylamine, were obtained from Fluka. *N*-(2-hydroxyethyl)piperazine-*N*-(2-ethanesulfonic acid) (HEPES), EDTA, potassium iodide (KI), sodium azide (NaN_3), urea, $CuCl_2{\cdot}2H_2O$, methanol and dimethyl sulfoxide (DMSO) were purchased from Sinopharm Chemical Reagent Co., Ltd. (Shanghai, China). Ethidium bromide (EB), methyl green, and 4′,6-diamidino-2-phenylindole (DAPI), calf thymus DNA (ct-DNA), Plasmid pBR322 DNA, superoxide dismutase (SOD) and catalase (from bovine liver) were purchased from Sigma-Aldrich. Sample solutions for DNA cleavage tests were prepared according to the standard sterile procedures in order to avoid ribonuclease contamination. HEPES buffer solution (50 mM, pH 7.40) was prepared by dissolving an appropriate amount of reagent HEPES in water, and used as solvent in spectroscopic measurements and DNA cleavage experiments. Concentrated stock solutions of the ligands and the complexes were prepared by dissolving each compound in methanol, which were diluted with the buffer to the required concentrations when used in the experiments. All aqueous solutions were prepared using doubly-distilled water, and degassed by ultrasonic deaeration and then sparged with nitrogen gas for 10 min to remove the dissolved gasses prior to use.

2.2. Physical measurements and analysis

Electrospray ionization mass data were acquired on a Finnigan LCQ electron spray mass spectrometer, and the isotopic distribution patterns for the synthesized complexes were simulated using the Isopro 3.0 program [58]. ^{1}H NMR spectra were recorded on a Bruker DRX-500 spectrometer at 293 K. Elemental analyses for C, H and N were performed on a Perkin-Elmer 240C elemental analyzer. Infrared spectra were recorded on a Bruker VECTOR22 spectrometer as KBr disks in the range of 4000–500 cm^{-1}. UV/Vis and Fluorescence spectra were respectively recorded on a Shimadzu UV-2450 spectrophotometer and a Jasco FP-6500 spectrofluorometer equipped with a temperature-controlled unit with quartz cuvettes (1.0 cm). The pH measurement and potentiometric titrations were carried out on a PHS-3C exact digital pH meter equipped with Phonix Ag-AgCl reference electrode (Cole-Parmer Instrument Co.). The gel imaging was assessed using Labworks Imaging and Analysis Software (UVP, Inc., Upland, CA).

2.3. Syntheses

Ligand, $\mathbf{L^1}$, was synthesized by the literature method described previously by us [55]. Its characterization results were presented in the Supplementary materials (Fig. S1–S4 and S6). $\mathbf{L^2}$ was obtained by reacting 2 equiv. of 2-{[2-(2-hydroxyethylamino)-ethylimino]-methine}-phenol with 1 equiv. of 2,6-bis(chloromethyl)-4-methylphenol in absolute tetrahydrofuran in the presence of triethylamine. The specific synthetic procedures are as follows. Triethylamine (2.02 g, 20 mmol) was added to 2,6-bis(chloromethyl)-4-methylphenol (2.05 g, 10 mmol) in dry tetrahydrofuran (25 mL) under stirring. The solution was cooled to 273 K and 2-{[2-(2-hydroxyethylamino)-ethylimino]-methine}-phenol (4.00 g, 20 mmol) was dropped into the mixture. The formed precipitate of triethylamine salt was removed by filtration after stirring for 5 days at room temperature. Concentration of the filtrate under reduced pressure gave oily syrup, which was washed with mixture of chloroform and dichloromethane, and dispersed in ethanol by vigorous stirring. Solution of concentrated HCl acid was added to the mixture till its final concentration reached 5 M, which was kept still for *ca.* 2 h to yield a yellowish semisolid product. $\mathbf{L^2}$ was obtained as its solid hydrochloride salt ($\mathbf{L^2}{\cdot}4HCl$) by recrystallisation of the raw product from ethanol containing minimum water in a yield of 37%. ^{1}H NMR (D_2O): δ 7.193 (s, 2H), 3.810–3.731 (m, 4H), 3.365–3.323 (m, 4H), 3.221–3.146 (m, 4H), 2.178–2.160 (d, J = 9.0, 4H) ppm (Fig. S8). ESI-MS found for $[C_{17}H_{32}N_4O_3 + H]^+$ (m/z): 341.1 (calcd. 341.25) (Fig. S9). Elemental analysis found (calcd.) (%): C, 41.73 (41.98); H, 7.40 (7.46); N, 11.40 (11.52). FT-IR spectra (ν, cm^{-1}): 3377.35 (br, s), 2967.00 (br, m), 1605.09 (m), 1488.11 (s), 1224.32 (m), 1166.35 (w), 1074.85 (m), 896.71 (w), 876.84 (w), 776.64 (w), 570.19 (br, w) (Fig. S10).

2,6-Bis(chloromethyl)-4-methylphenol was prepared according to the reported procedures [59], which should be stored in a sealed container at −20 °C. The intermediate 2-{[2-(2-hydroxyethylamino)-ethylimino]-methine}-phenol was prepared by condensing 2-(2-aminoethylamino)-ethanol and salicylaldehyde in methanol at refluxing temperature. The synthetic routes to $\mathbf{L^1}$ and $\mathbf{L^2}$ are illustrated in Scheme 1.

The dinuclear copper(II) complexes **1** and **2** were prepared by the general complexation techniques following the same procedures. A sample of 2 equiv. of $CuCl_2{\cdot}2H_2O$ in methanol (25 mL) was slowly dripped into a methanolic solution containing 1 equiv. of $\mathbf{L^1}$ or $\mathbf{L^2}$ (10 mL) in the presence of 2 equiv. of triethylamine. The resulting mixture was stirred for 10 min at room temperature and then refluxed for 1 h. The blue solid formed was collected and then washed with dry methanol for three times. Microcrystals were obtained by recrystallizing the solid in water/methanol (1/2, v/v), which were dried overnight *in vacuo* (yield: 70% for **1** and 65% for **2**) and characterized (see the following sections and Supplementary materials).

2.4. Potentiometric measurements

Equilibrium constants for the protonation/deprotonation of the ligands and the prepared dinuclear complexes, and the complexation

reactions of the ligands with Cu(II) in aqueous solution were all determined by pH potentiometric titrations over the pH range 3–11 at 298.1 ± 0.1 K using a pH meter fitted with a Phonix Ag-AgCl combination electrode, calibrated to read –log[H^+] directly (designated as pH), according to the recommended method [60]. During the titrations, the ionic strength was kept constant at 0.10 M by the addition of NaCl. The stability of the combined glass electrode was checked by a calibration titration prior to and after each measurement using 0.01 M CO_2-free standard NaOH solution to titrate known volume of a 0.01 M standard HCl solution containing the same background electrolyte at 298.0 ± 0.1 K, and the pK_w value was taken to be 13.76. All measurements were conducted on stirred solutions in a water-jacketed cell at 298.0 ± 0.1 K. The total sample volume in all cases was 20.0 mL, and dinitrogen was slowly bubbled through the sample solutions to ensure the absence of oxygen and carbon dioxide.

For measuring the protonation/deprotonation equilibria of the ligands $\mathbf{L^1}$ and $\mathbf{L^2}$, the methanol/water (1/1, v/v) solution of each ligand (2.0 mM) containing 0.10 M NaCl in the thermostated cell were previously acidified (pH ≤ 3) with 0.10 mM HCl solution. Individual measurement datum was collected by incremental addition (2–10 μL) of 0.10 M standardized NaOH solution to each solution after *ca* 5–10 min equilibration under constant stirring. The titrations were performed for each sample in triplicate, and the averages were taken as the final results. For measuring the deprotonation equilibria of the complexes **1** and **2**, each complex (2.0 mM) was directly dissolved in the aqueous methanol solution containing 0.10 M NaCl and titrated with the standardized NaOH solution by the same procedures. The equilibrium constants for the protonation/deprotonation of the ligands and the complexes were determined from analysis of the titration data.

Complexation equilibrium measurements of $\mathbf{L^1}$ and $\mathbf{L^2}$ towards Cu (II) ions were conducted on the methanol/water (1/1, v/v, 0.10 M NaCl) solutions containing each ligand and $CuCl_2{\cdot}2H_2O$ in molar ratios of **L**/Cu(II) ranging from 1:1 to 1:2, previously acidified with 0.10 mM HCl solution at pH ≤ 3, by the same procedures described above. The solution of $CuCl_2{\cdot}2H_2O$ was calibrated by standard EDTA prior to use. The complexation equilibrium constants were determined using the triplicates by the BEST program [61], and the species distributions were obtained from the calculated formation and protonation constants by the SPE and SPEPLOT9 programs [61]. All equilibrium constants were calculated as concentration constants.

2.5. DNA binding

All experiments relevant to interactions of the complexes **1** and **2** with ct-DNA were conducted in 50% methanol aqueous HEPES buffer (50 mM, pH 7.40) containing 50 mM NaCl at 310 ± 0.2 K. The ct-DNA stock solution was prepared by dissolving appropriate amount of ct-DNA in the buffer solution and was dialyzed against the same buffer overnight. The solution was examined on the UV/Vis spectrophotometer giving UV absorbance ratios at 260 and 280 nm above 1.8, which indicates that the ct-DNA was sufficiently free of protein [62]. DNA concentration per nucleotide was determined by absorption spectroscopy after proper dilution with water using the molar absorption coefficient 6600 $M^{-1}\,cm^{-1}$ at 260 nm [63]. The ct-DNA stock solution was stored at lower than 277 K and used within 4 days. The complexes **1** and **2** were respectively dissolved in the above buffer and titrated with the aqueous ct-DNA solution (2.5 mM). The changes in absorbance at 239.6 nm for **1** and 241.0 nm for **2** with increasing amounts of ct-DNA were recorded with the buffer as a reference. From the absorption titration data, the intrinsic binding constant (K_b) of the copper(II) complexes with ct-DNA was respectively determined by the Wolfe–Shimer Eq. (1) [64],

$$\frac{[DNA]}{\varepsilon_a - \varepsilon_f} = \frac{[DNA]}{\varepsilon_b - \varepsilon_f} + \frac{1}{K_b(\varepsilon_b - \varepsilon_f)} \quad (1)$$

where [DNA] is the concentration of DNA in the base pairs, and ε_a, ε_f and ε_b are the apparent (A_{obsd}/[Complex]), the free and the fully bound complex extinction coefficients, respectively. A plot of [DNA]/($\varepsilon_a - \varepsilon_f$) *versus* [DNA] with a slope of 1/($\varepsilon_b - \varepsilon_f$) and an intercept of 1/[K_b(ε_b - ε_f)] gives K_b as the ratio of slope to the intercept.

The fluorescence spectra were recorded at room temperature (λ_{ex} = 510 nm, λ_{em} = 605 nm). The experiment was carried out by titrating aliquots of each complex (25 μM) dissolved in the HEPES buffer (50 mM, pH 7.40, 50 mM NaCl) into the aqueous EB-ct-DNA solution containing 25 μM EB and 25 μM ct-DNA.

2.6. DNA cleavage and mechanism studies

Supercoiled pBR322 plasmid DNA was used as a substrate to assay cleavage activity of the complexes **1** and **2** by agarose gel electrophoresis at 310 K as previously described [65]. The cleavage was evaluated by monitoring the conversion of the closed circular supercoiled plasmid DNA form (Form I) to the nicked circular form (Form II, single strand breakage), and then to the linear form (Form III, double strand breakage). HEPES buffer (50 mM, pH 7.40) containing 10% methanol (v/v) was used to prepare each complex solution. In general, 2 μL of pBR322 DNA (0.1 μg μL^{-1}) was syringed into 6 μL of **1** or **2** solution (15 μM), and 3 μL of ascorbic acid (Vc) in 100-fold molar excess of the complex was added to each solution, which was incubated at 310 K for an appropriate time under aerobic conditions. Then, 4 μL of solution containing 30% glycerol, 0.25% bromophenol blue, 0.25% xylene cyanole and EDTA (5 mM) was added to the mixture to quench the cleavage process. The solution was then subjected to electrophoresis on 0.7% agarose gel in TAE buffer (40 mM Tris-acetate, 1 mM EDTA) at 80 V. After electrophoresis, the different DNA forms were visualized by fluorescence imaging of EB under UV light and photographed. The data analysis was performed using Bio-Rad's Image Lab Software (Version 3.0). In all cases, the background fluorescence was subtracted and a correction factor of 1.47 was used for Form I DNA assessment due to a smaller affinity of the supercoiled Form I of plasmid DNA to EB [66]. All experiments were performed in triplicate and the average was adopted as the final results.

To examine the reactive oxygen species (ROS) possibly involved in the DNA cleavage promoted by **1** and **2**, pBR322 DNA was incubated with appropriate amount of ROS inhibitors including hydroxyl radical scavengers (DMSO, KI and urea) [67], singlet oxygen quenchers (NaN_3) [68], superoxide scavenger (SOD) [69], and hydrogen peroxide scavenger (catalase) [66] in the buffer for 30 min at 310 K. Then, appropriate amount of each complex and Vc was added, and incubated for 1 h at the same temperature. The mixture was then diluted with the HEPES buffer to 20 μL, and subjected to gel electrophoresis as described above. For anaerobic DNA cleavage assays, the deoxygenated water was prepared according to the known method elsewhere, and the assay was conducted referring the procedures reported in literature [65].

3. Results and discussion

3.1. Synthesis

The phenol-based ligands studied in this work, $\mathbf{L^1}$ and $\mathbf{L^2}$, have two dissimilar compartments with N_4O_3 metal-binding sites sharing a central phenolic oxygen atom in each molecule. Syntheses of $\mathbf{L^1}$ and $\mathbf{L^2}$ have been achieved by a nucleophilic reaction of 2 equiv. of secondary amine intermediates with 1 equiv. of 2,6-bis(chloromethyl)-4-methylphenol in the presence of triethylamine as a base in anhydrous tetrahydrofuran at ambient temperature. The synthetic pathway used to obtain both ligand**s** is depicted in Scheme 1. In the case of $\mathbf{L^2}$, the primary amine group of 2-(2-aminoethylamino)ethanol was pre-protected by salicylaldehyde, and then deprotected in 5 M HCl aqueous solution after reaction with 2,6-bis(chloromethyl)-4-methylphenol. Their characterization data are detailed in the experimental section and presented in the Supplementary materials. $\mathbf{L^1}$ has been successfully

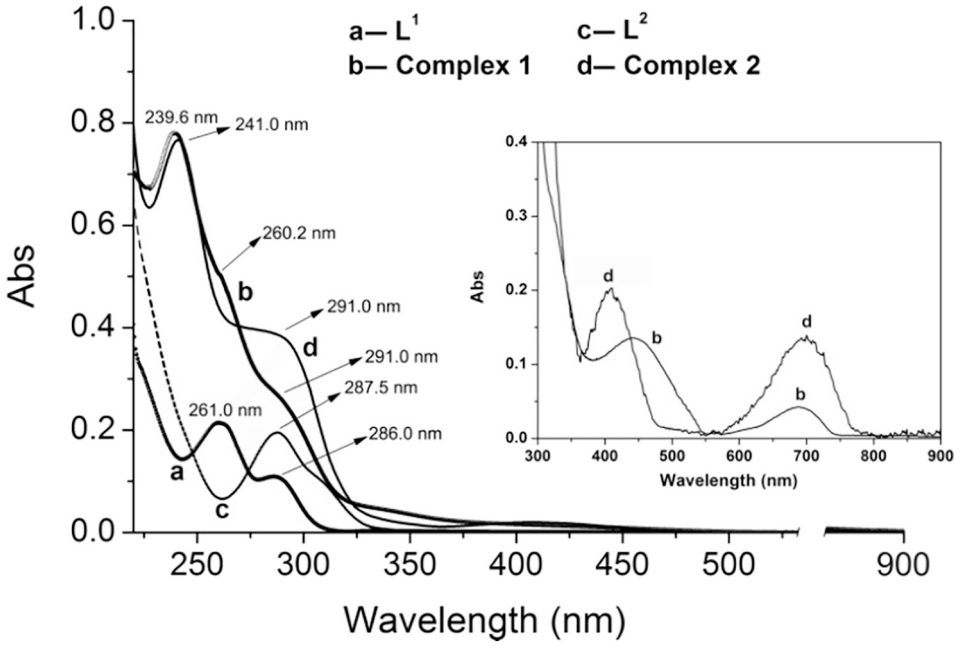

Fig. 1. UV–Vis spectra of complexes **1** and **2** and the corresponding ligands dissolved in HEPES buffer (50 mM, pH 7.40) containing 50% methanol and 50 mM NaCl at 298 K.

used in the assembly of a dinuclear Zn(II) complex to model phosphodiesterase in our previous study [55]. In this work, we use $\mathbf{L^1}$ and the homologous ligand $\mathbf{L^2}$ to offer a direct comparison of aryl- with alkyl-N donors in constructing dinuclear copper(II) complexes for evaluating their nuclease-like activity. The dinuclear copper(II) complexes with general formula of $[Cu_2(H_{-1}L)]^{n+}$ ($H_{-1}L$ denotes the monodeprotonated form of the ligands) were synthesized by mixing methanolic solution containing each ligand and $CuCl_2{\cdot}2H_2O$ in a stoichiometric ratio of 1: 2 under reflux conditions. The complexes are crystalline, slightly hygroscopic solids, and soluble in commonly polar organic solvents and almost soluble in water. The ESI mass spectra of the aqueous methanolic solutions of the synthesized complexes (**1** and **2**) show the presence of the dinuclear copper(II) unit, indicating the stability of the dicopper(II) frameworks at room temperature. Moreover, polymer formation was not observed using the present ligands even at high pH. Unfortunately, attempts to isolate single crystals of the complexes **1** and **2** suitable for X-ray crystal structure determination have been unsuccessful to date, and so they were characterized by various routine techniques.

3.2. FTIR and UV/Vis spectroscopy

The complexes **1** and **2** were initially characterized by infrared spectroscopy as presented in the Supplementary materials (Fig. S5 and S11). Each free ligand clearly shows a strong broad band around 3377 cm^{-1}, which is assigned to the ν(OH) vibration of the phenolic group [70]. The broadness is due to intermolecular hydrogen bonding between the phenolic and the tertiary amino groups. The ν(O—H) vibration of alcoholic groups in each ligand may be overlapped completely with this band due to the additional intermolecular or intramolecular hydrogen bonding between the alcoholic groups themselves [71]. However, a broad band between 2500 cm^{-1} and 3300 cm^{-1}, typical of O—H stretching, was still observed in the spectrum of each ligand. The two complexes **1** and **2** show the expected characteristic skeletal stretching vibration bands for aromatic groups (phenyl C═C and/or pyridyl C═N) in the range of 1606–1611 cm^{-1} in respective spectrum. The ν(O—H) band of the phenolic group of free ligands around 3377 cm^{-1} disappears, which accounts for complexation of the phenolic oxygen with Cu(II) ions *via* deprotonation [70]. A moderate band at 1552.68 cm^{-1} for **1** and 1583.89 cm^{-1} for **2** was observed respectively, which can be assigned to the bridging phenoxide based on the reported studies [72]. This inference is confirmed by shifts of the phenolic (C—O) stretching vibrations for **1** from 1478.75 cm^{-1} and 1435.43 cm^{-1} (free $\mathbf{L^1}$) to higher frequency at 1481.63 cm^{-1} and 1468.29 cm^{-1}, and for **2** from 1457.71 cm^{-1} (free $\mathbf{L^2}$) to 1474.21 cm^{-1}, similar to the other dinuclear copper(II) complexes derived from analogous ligands [73]. A new strong band centerd at 3423.67 cm^{-1} for **1** and 3400.19 cm^{-1} for **2** was observed, respectively, which could be attributed to ν(O—H) vibration of the coordinated μ-hydroxo group [74]. The significant absorption shifts to lower frequency could be explained that the alkylhydroxyl and alkylamino groups in the complex molecules are highly susceptible of formation of hydrogen bonding between each other [75], particularly for **2** featuring two alkylhydroxyls and two alkylaminos. The ν(O—H) vibration of the alcoholic groups in each complex may likewise merges with this band. However, the bands at 1052.26 cm^{-1} for $\mathbf{L^1}$ and 1074.85 cm^{-1} for $\mathbf{L^2}$ assignable to ν(C—O) of the alcoholic groups undergo notable shift to 1030.20 cm^{-1} and 1058.81 cm^{-1} respectively, and their intensity significantly attenuate upon complexation with Cu (II) ions, suggesting coordination of the alcoholic groups to Cu(II) ions. Moreover, the signal around 1593 cm^{-1} assigned to ν(C═N) vibration of the pyridyl groups in $\mathbf{L^1}$ undergoes a shift towards higher energy band at approximately 1606 cm^{-1} upon complexation, indicating coordination of the pyridyl-N donor to Cu(II) ions in complex **1**. A strong broad band centered at 2967 cm^{-1} present in $\mathbf{L^2}$ is probably attributed to the symmetric and asymmetric ν(N—H) vibration of the alkylamino groups, which appears in a lower frequency region likely due to the strong intermolecular or intramolecular hydrogen bonding between the amino groups themselves or between the amino and the alcoholic groups in the ligand. Upon complexation, the position of this band is significantly shifted to higher frequency at approximately 3234 cm^{-1}, suggesting the amino groups may partially lose hydrogen bonding and coordinate to Cu(II) [17]. From comparison of the FTIR spectrum of each ligand and the corresponding complex, the coordination of Cu(II) ions to each ligand can be concluded, since the main bands present in each ligand have changed observably upon complexation.

Each concentrated methanolic stock solution of $\mathbf{L^1}$, $\mathbf{L^2}$ and the corresponding complexes **1** and **2** was diluted with methanol/HEPES buffer

(1/1, v/v, 50 mM, pH 7.40) affording appropriate concentration, and their electronic spectra were recorded at 298 K over a range of 200–700 nm with the buffer solution as a reference. As shown in Fig. 1, $\mathbf{L^1}$ displays characteristic bands with λ_{max} at 261.0 nm ($\varepsilon = 3.52 \times 10^3\ M^{-1}\ cm^{-1}$) and 286.0 nm ($\varepsilon = 1.48 \times 10^3\ M^{-1}\ cm^{-1}$), and $\mathbf{L^2}$ shows a band with λ_{max} at 287.5 nm ($\varepsilon = 1.02 \times 10^3\ M^{-1}\ cm^{-1}$), respectively. The band centered at 261.0 nm for $\mathbf{L^1}$ is assigned to the absorption of the pyridyl group, whereas the bands around 286.0 nm for $\mathbf{L^1}$ and 287.5 nm for $\mathbf{L^2}$ could be associated with overlapping of the phenol group in its neutral ($\lambda_{max} \approx 261.0$ nm) and anionic ($\lambda_{max} \approx 235$ nm and 292 nm) forms based on the previous studies [19,76]. A band with λ_{max} at *ca.* 239.6 nm ($\varepsilon = 6.15 \times 10^3\ M^{-1}\ cm^{-1}$) together with a shoulder at *ca.* 291.0 nm for **1**, and a band with λ_{max} at *ca.* 241.0 nm ($\varepsilon = 3.85 \times 10^3\ M^{-1}\ cm^{-1}$) along with a shoulder at *ca.* 291.0 nm for **2** is observed respectively, which are attributed to the intraligand $\pi \rightarrow \pi^*$ charge transfer transitions of the phenolate group engaged in the coordination of Cu(II) [59], since two bands with λ_{max} at 235–243 nm and 291–295 nm are universally characteristic for the presence of the anionic phenolate function [19,76]. In addition, a weak broad absorption centered at 406 nm ($\varepsilon = 101.3\ M^{-1}\ cm^{-1}$) is observed for complex **2**, which can be ascribed to the bridging phenoxo-Cu(II) charge transfer (LMCT) transitions [59,77,78], similar to the related μ-phenoxo dicopper(II) complexes [20]. The spectrum of **1** resembles that of **2** exhibiting a weaker broad band centered at 449 nm ($\varepsilon = 98.1\ M^{-1}\ cm^{-1}$), which may also be assigned to a LMCT between the phenolate and Cu(II) ions. This spectral feature suggests that in solution an equilibrium between the protonated and deprotonated forms of the coordinated phenol group is most probably taking place [40]. Taking account that a hydroxido-Cu(II) LMCT was likewise observed in the region of 350–400 nm [76], this band may also arise from the combination of the phenoxido-Cu(II) and hydroxido-Cu(II) LMCT. The absorption at longer wavelengths than 600 nm attributed to Cu(II) d–d transition [23] was observed respectively for **1** and **2** (690 nm for 1 and 701 nm for 2) (See inset in Fig. 1).

The stability of the complexes **1** and **2** in 50% methanol HEPES buffer was further examined by **UV**–Vis spectroscopy. The UV/vis spectrum of each complex in the buffer solution was monitored at 298 K in a period of 24 h with an interval of 4 h for comparison (see Fig. S7 and S13 in the Supporting materials). The results did not reveal appreciable changes in either the intensity or the position of the absorption bands along that period, suggesting the complexes under study are stable in aqueous solutions for at least the duration.

3.3. Mass spectral characterization and stability of the dinuclear copper(II) species

The formation of dinuclear phenolate copper(II) complexes of $\mathbf{L^1}$ and $\mathbf{L^2}$ in the case of Cu(II) in excess was confirmed by electrospray ionization mass spectrometry (ESI-MS). The complexes **1** and **2** were dissolved respectively in CH_3OH/H_2O (1/1, v/v) solution and then subjected to ESI-MS analysis. The relevant copper(II) species were positive complex cations throughout, and no negatively charged species were detected. As shown in Fig. 2, the ESI-MS spectra of **1** and **2** display general characteristic features which provide qualitative information about their compositions. The spectrum of **1** shows one dominant peak at $m/z = 298.1$ amu (100%) with a separation of 0.5 unit, indicating a doubly charged species which may be attributed to a chloride anion present $[Cu_2(H_{-1}\mathbf{L^1})(Cl)]^{2+}$ (Calcd. $m/z = 298.04$) based on the analysis for the isotopic distribution profiles of the calculated and experimental spectra (see Fig. 2 inset). Another weak peak at 595.2 amu (20%) with a separation of 1 unit was also detected and may be assigned to $[Cu_2(H_{-1}\mathbf{L^1})(OH)_2]^+$ (Calcd. $m/z = 595.10$ amu). The theoretical isotope patterns calculated for the respective empirical formula $Cu_2C_{25}H_{31}N_4O_3Cl$ and $Cu_2C_{25}H_{33}N_4O_5$ are in good agreement with the experimentally found ones. The results for complex **2** show three major mass peaks at $m/z = 250.0$ (100%), 499.0 (50%) and 535.2 amu (25%). The peak separation of the first one is again 0.5 unit, indicating a doubly charged fragment probably assignable to a solvate water present dicopper(II) complex $[Cu_2(H_{-1}\mathbf{L^2})(OH)(H_2O)]^{2+}$ (Calcd. $m/z = 250.06$). The other two isotopic patterns exhibit peak separations of 1 unit, suggesting singly charged species which could be assigned as $[Cu_2(H_{-1}\mathbf{L^2})(OH)_2]^+$ (Calcd. $m/z = 499.10$) and $[Cu_2(H_{-1}\mathbf{L^2})(Cl)(OH)(H_2O)]^+$ (Calcd. $m/z = 535.08$), respectively. The simulated isotopic patterns of each ion peak also show a close resemblance to the corresponding experimental spectra. In summary, the ESI-MS spectra unambiguously demonstrate that the complexes **1** and **2** exist as dicopper (II) species in aqueous solution. The assignments of the peaks observed in the ESI-MS spectra for **1** and **2** in CH_3OH/H_2O (1/1, v/v) solution are given in Table 1.

The ability of $\mathbf{L^1}$ and $\mathbf{L^2}$ to chelate Cu(II) ion *in situ* and to stabilize the dinuclear frameworks in aqueous systems was further examined by ESI-MS. Upon addition of 2 equiv. of Cu(II) into 1 equiv. of $\mathbf{L^1}$ or $\mathbf{L^2}$ in methanol/water solution (1/1, v/v) respectively, an instant color change from light yellow to turquoise was observed, indicating that each ligand instantaneously binds to Cu(II) ions in aqueous solution. The mixture was heated at *ca.* 335 K and subjected to ESI-MS analysis at every 20 min during initial 2 h, and afterwards at 4 h intervals within a period of 24 h. The results showed that the dinuclear copper(II) complex of each ligand is almost completely generated after *ca.* 1 h of reaction. Moreover, appreciable change in peak intensity was hardly observed after 1 h, indicating the stability of the resultant dinuclear species in the aqueous solution for at least 24 h.

3.4. Equilibrium studies

3.4.1. Protonation equilibria of ligands and dicopper(II) complexes

The pK_a values of ligands $\mathbf{L^1}$ and $\mathbf{L^2}$ were firstly determined by means of pH potentiometric titrations in 50% methanol aqueous solution at a constant ionic strength (0.10 M NaCl). Initially, an excess of HCl solution (0.1 M) was added to the samples in order to start the measurements from acidic conditions, where all four donor atoms of each ligand (2.0 mM) are protonated. After neutralization of the strong acid, the potential labile protons at the donor atoms were sequentially deprotonated as shown in Fig. 3. The equivalence points were determined by fitting of the titration profiles using a Boltzman model, and the values of acid dissociation constant (K_a) for the deprotonation reactions were measured from the titration curves at half-equivalence points where $pH = pK_a$ as given in Table 2. In the curve of $\mathbf{L^1}$, three inflection points corresponding to three kinds of active hydrogen are observed although $\mathbf{L^1}$ has an acidic phenol proton and a total four potential protonatable sites. Fitting of the curve gives rise to pK_a values of 4.46, 8.36 and 10.13. The dissociated proton number for the respective deprotonation step was calculated, from the consumption equivalence of the standardized NaOH solution, to be just 2, approximately 2 and 1, respectively. Analysis of the pK_a values revealed that the three deprotonation reactions occur on different sites of $\mathbf{L^1}$ molecule. The protonation/deprotonation equilibria of $\mathbf{L^1}$ have been previously studied in CH_3CN/H_2O at ionic strength of 0.1 M Et_4ClO_4 by Gahan et al. [22] displaying three titratable protons corresponding to pK_as of 4.4, 7.7, and 11.6, among which the first two pK_a were proposed to be associated with the deprotonation of the pyridinium and the third one was assigned to the pendent alcohol, respectively. In the elegant studies of Tóth et al. [79] and Nordlander et al. [80], however, the protonation/deprotonation equilibria for the pyridyl nitrogen atoms in aminocarboxylate-containing "end-off" compartmental ligands were not observed in aqueous solution. Taking into account that the pK_a value of the conjugate acid of a free pyridine ranges between 5.15 and 5.30 [81], we suppose that under our experimental conditions for $\mathbf{L^1}$ the first pK_a is due to dissociation of the protonated pyridyl nitrogen donors. The second pK_a of $\mathbf{L^1}$ may be attributed to deprotonation of the protonated aliphatic tertiary amino groups. The value is comparable to those of the recently reported for the compartmental

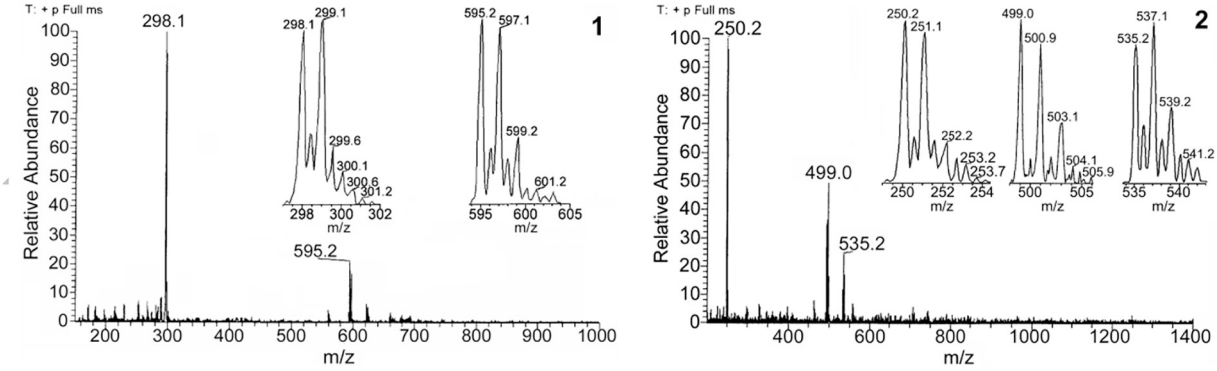

Fig. 2. ESI-MS spectra (positive) and simulated isotopic patterns of the complexes **1** and **2** in CH_3OH/H_2O (1/1, v/v) solution.

Table 1
Assignments of the peaks observed in the ESI-MS spectra for the complexes **1** and **2** in CH_3OH/H_2O (1/1, v/v) solution (see Fig. 2).

Complex	Obs. *m/z*	Assigned species	Formula	Calc. *m/z* (Exact mass)
1	298.1	$[Cu_2(H_{-1}\mathbf{L^1})(Cl)]^{2+}$	$Cu_2C_{25}H_{31}N_4O_3Cl$	298.04
	595.2	$[Cu_2(H_{-1}\mathbf{L^1})(OH)_2]^{+}$	$Cu_2C_{25}H_{33}N_4O_5$	595.10
2	250.2	$[Cu_2(H_{-1}\mathbf{L^2})(OH)(H_2O)]^{2+}$	$Cu_2C_{17}H_{34}N_4O_5$	250.06
	499.0	$[Cu_2(H_{-1}\mathbf{L^2})(OH)_2]^{+}$	$Cu_2C_{17}H_{33}N_4O_5$	499.10
	535.2	$[Cu_2(H_{-1}\mathbf{L^2})(Cl)(OH)(H_2O)]^{+}$	$Cu_2C_{17}H_{34}N_4O_5Cl$	535.08

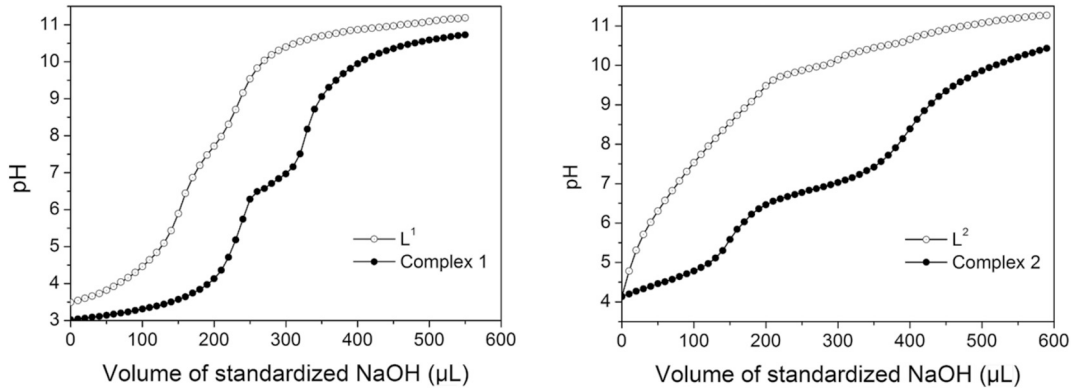

Fig. 3. Potentiometric titration curves of the ligands $\mathbf{L^1}$ and $\mathbf{L^2}$ (2.0 mM) and the complexes **1** and **2** (2.0 mM) in methanol/water (1/1, v/v; 0.10 M NaCl) at 298 ± 0.1 K.

Table 2
pK_a values potentiometrically determined for ligands $\mathbf{L^1}$ and $\mathbf{L^2}$, and complexes **1** and **2** in 50% methanol aqueous solution (298 ± 0.1 K, I = 0.10 M NaCl) together with some structurally-related dicopper(II) complexes for comparison.*

Compound	pK_{a1}	pK_{a2}	pK_{a3}	Ref.
L^1	4.46	8.36	10.13	this work
L^2	7.51	9.83	10.44	this work
Complex 1	3.39	6.71		this work
Complex 2	4.59	6.99	7.84	this work
$[Cu_2(L)(H_2O)_2(ClO_4)_2]^{+}$		6.10	8.15	12
$[Cu_2(L)Cl_3]$		4.60	7.16	85
$[Cu_2(BPMP)(OH)]^{2+}$		4.95	12.0	86
$[Cu_2(HL)(\mu\text{-}OCH_3)]^{2+}$		5.23	7.59	60
$[Cu_2(L_{OCH3})(\mu\text{-}OH)]^{2+}$		5.3	12.0	41
$[Cu_2(L_F)(\mu\text{-}OH)]^{2+}$		5.15	12.1	41
$[Cu_2(L_{CF3})(\mu\text{-}OH)]^{2+}$		5.45		41
$[Cu_2(L)(\mu\text{-}OH)]^{2+}$		6.10		65
$[Cu_2L(\mu\text{-}OH)]^{2+}$		4.3		84

* pK_{a2} and pK_{a3} for the referred complexes correspond to the aquo/μ-hydroxo and aquo/terminal hydroxo protonation/deprotonation equilibrium, respectively.

polyaminocarboxylate ligands (pK_{a1} = 7.79–8.11, pK_{a2} = 8.44–8.74) [79]. In particular, the pK_{a2} value of $\mathbf{L^1}$ is approximately one logarithmic unit lower than those determined potentiometrically for the conjugate acids of free aliphatic tertiaryamines containing an ethylhydroxyl, *e.g.* diethylethanolamine (pK_a = 9.75) [82,83] and dimethylethanolamine (pK_a = 9.22) [83]. This could be explained by the presence of a N-linked pyridino moiety in $\mathbf{L^1}$ capable of decreasing the basicity of the exocyclic nitrogens revealed by Tóth et al. [79]. In addition, this difference may still be ascribed to the effect of intramolecular hydrogen bonding between the tertiary amino-N and the cresol in $\mathbf{L^1}$, in which the acidic cresol hydroxyl proton as a hydrogen-bond donor is shared by the tertiary amino and pyridyl groups *via* intermolecular hydrogen bonding as found in similar ligands [19]. This case may influence the availability of the tertiary amino-N atoms for protonation, and accordingly make the dissociation of the protonated amine(s) easier. The third pK_a may be assigned to the deprotonation of phenolic hydroxyl in terms of the dissociation constant of free phenol (pK_a = 10) [81].

In the case of $\mathbf{L^2}$, also three titratable protons are observed under the experimental conditions employed, which correspond to pK_as of 7.51, 9.83 and 10.44. The dissociated proton number for each deprotonation step was calculated to be approximately 2, 1 and 1, respectively. The

pK_{a1} may be related to the protonation/deprotonation equilibrium of the tertiary amines in $\mathbf{L^2}$. This value is approximately one logarithmic unit lower than pK_{a2} determined for $\mathbf{L^1}$, while is comparable to pK_{a1} for the polyaminocarboxylate ligands (pK_{a1} = 7.79–8.11, pK_{a2} = 8.44–8.74) [79]. In particular, the value of pK_{a1} is still rather low in comparison with those for the conjugate acids of free diethylethanolamine (pK_a = 9.75) [82,83] and dimethylethanolamine (pK_a = 9.22) [83]. This may be ascribed to the combined effects of involvement of the cresol hydrogen-bond interactions as discussed above, and the strong electrostatic repulsion of the protonated primary amine functions present in $\mathbf{L^2}$. The last two pK_a values are very close and rather high, suggesting the two deprotonation steps involve similar sites located far from each other. The values are found to lie in the pK_a ranges corresponding to acid dissociation equilibria of the protonated primary amine functions linked to a phenolate group [19,76]. Furthermore, the pK_a value of the conjugate acid of free ethyl-1,2-diamine is 10.65, and that of free ammonium is known to generally range between 9 and 10 [81]. Taking into account these known values together with the higher flexible topology of $\mathbf{L^2}$ moleucule, we can suppose that under our experimental conditions the protons corresponding to pK_{a2} and pK_{a3} are located at the two primary amino nitrogen atoms. In the present study, deprotonation equilibrium of the phenolic hydroxyl of $\mathbf{L^2}$ was not discerned under the experimental conditions, probably due to overlapping in the protonation/deprotonation equilibria of the primary amine functions.

The deprotonation equilibria of the complexes **1** and **2** were likewise measured potentiometrically on the aqueous methanol solution (methanol/water = 1/1, v/v, 0.10 M NaCl) containing each complex (2.0 mM) without previous acidification. The titration curves for the complexes are presented in Fig. 3 and the deprotonation equilibrium steps are proposed in Scheme 2. It is noted that a precipitate was observed for **1** and **2** above pH 11.1 and 11.5 in measurements, respectively; thus, data above this pH do not correspond exclusively to solution equilibria.

Potentiometric titrations of **1** and **2** show the neutralization of approximate 3 and 4 mol of NaOH per mole of each complex in the pH range of 3–11. Fitting the data results in the pK_a of 3.39 and 6.71 for **1**, and 4.59, 6.99 and 7.84 for **2**, respectively. When the complexes **1** and **2** are dissolved in aqueous solution, facile dissociation of possibly exogenously-bridged or/and weakly-bound ligand(s) with replacement by water molecules to produce aqua dicopper(II) intermediates is expected. Considering the requirement of Cu(II) coordination and the donor sets provided by each ligand, the generation of diaqua dicopper(II) intermediates $[Cu_2(H_{-1}L)(H_2O)_2]^{3+}$ (**1**a and **2**a, Scheme 2) seems highly possible. Hydrogen ion is most likely to compete with Cu(II) for $\mathbf{L^1}$ and $\mathbf{L^2}$ binding in aqueous media, which leads to partial protonation of the donors with higher basicity. It should be uncontroversial that in the presence of metal ions the central phenolic –OH can be deprotonated even under acidic pH conditions [12]. Moreover, the consumption of the protons associated with the possibly protonated tertiary amino- and pyridyl-nitrogen atoms in $\mathbf{L^1}$ in the complexation with Cu(II) ions may be overlapped in the acid-base titrations. Therefore, there are no unambiguous assignment of the observed pK_{a1} for a specific protonation/deprotonation equilibrium but it is a composite of multiple pH-dependent equilibria. Anyway, for the complexes **1** and **2** the respective pK_{a1} possibly correlates with the dissociation equilibrium of the protonated donor atoms. The pK_{a2} of 6.71 for **1** and 6.99 for **2** is likely to be attributed to deprotonation of one of the coordinated water molecules from **1**b and **2**b with concomitant generation of a hydroxo-bridged species $[(H_{-1}L)Cu^{II}(\mu\text{-}OH)Cu^{II}(H_2O)]^+$ (**1**c and **2**c), respectively, evidenced by the ESI-MS spectral analysis, like the reported for a number of similar dicopper(II) complexes [12,41,60,65,84–86]. Typical pK_a values determined by spectrophotometry or potentiometry for the deprotonation of an aqua ligand bound to Cu(II) in a range of dicopper(II) complexes derived from phenol-based "end-off" compartmental ligands to generate hydroxo-bridged species are generally between 4.3 and 6.1 [12,41,60,65,84,87]. The pK_{a2} values of **1** and **2** are higher than those associated with the aquo/μ-hydroxo protonation equilibrium found in these dicopper(II) complexes, which implies the coordinated water molecule involved may be located at apical position rather than at the equatorial position of a Cu(II) ion in **1**b and **2**b, as the cases previously revealed in other copper(II) complexes [40]. Furthermore, it seems that the alkylamino or the alkylhydroxyl groups act as hydrogen bond acceptors to the Cu(II)-bound water molecule, thereby raising the pK_a value. The higher pK_{a2} values of the complexes also suggest that the potential donors in each ligand appear to bind strongly with Cu(II) ions, making the binding of water with Cu(II) weaker. In addition, the pK_{a2} value of **1** is lower than that of **2**, indicating that the Lewis acidity of **1** is stronger than **2**. This difference is presumably due to the tighter binding of $\mathbf{L^2}$ than $\mathbf{L^1}$ with Cu(II) given that the alkyl primary amino functionalities in $\mathbf{L^2}$ are more stronger electron-donating groups than the aromatic pyridyl ones in $\mathbf{L^1}$. Thus, it could be inferred that a decrease in the donor strength of a ligand correlates with an increased Lewis acidity of the metal-coordinated water. When pH of the solution is raised to 6.5, for complex **2** another deprotonation equilibrium with pK_a of 7.84 is observed, roughly in accordance with an aquo/hydroxo equilibrium measured for a copper(II)-bound water molecule in a number of structurally related dinuclear complexes such as $[Cu_2(L)Cl_3]$ (HL = 3-[(4,7-diisopropyl-1,4,7-triazacyclononan-1-yl)methyl]-2-hydroxy-5-methyl benzaldehyde) (pK_a = 7.16) [85], $[Cu_2(HLdtb)(\mu\text{-}OCH_3)]^{2+}$ (H_2Ldtb = {2-[Bis(2-pyridylmethyl)aminomethyl]-6-[(3,5-di-tert-butylbenzyl-2-hydroxy)(2-pyridylmethyl)]aminomethyl}-4-methylphenol) (pK_a = 7.59) [60], $[(BPBPMP)Fe^{III}(\mu\text{-}OH)Cu^{II}(OH_2)]^{2+}$ (H_2BPBPMP = 2-bis[{(2-pyridylmethyl)aminomethyl}-6-{(2-hydroxybenzyl)(2-pyridylmethyl)} aminomethyl]-4-methylphenol) (pK_a = 7.82) [88], $[Cu_2(TPPNOL)(OAc)(H_2O)]^{2+}$ (TPPNOL = N,N,N′-tris-(2-pyridylmethyl)-1,3-diaminopropan-

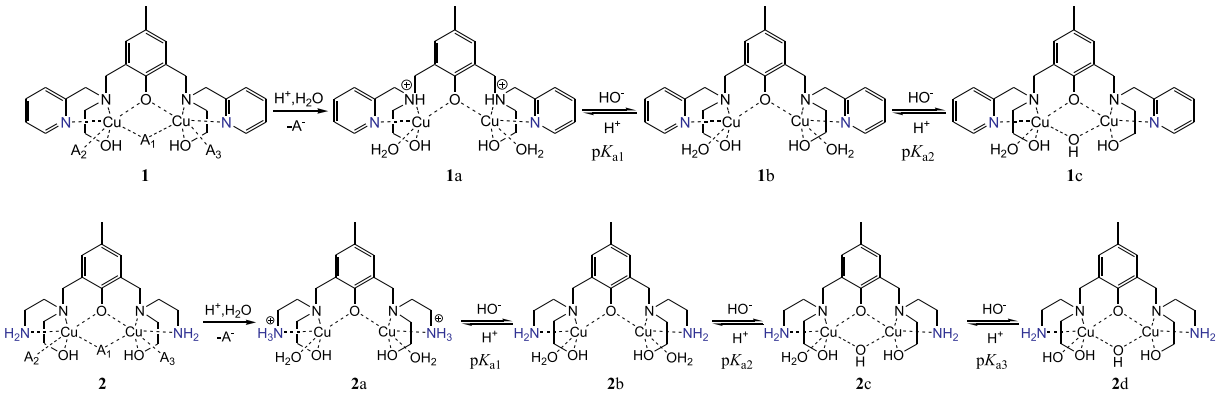

A_1, A_2 and A_3 in the complex molecules denote possible ancillary ligands including H_2O, Cl^- or OH^- based on the characterization results.

Scheme 2. Structrual representation of pH-dependent aqueous equilibria of **1** and **2.**

2-ol) (pK_a = 8.0) [89], and $[Cu_2(L)(H_2O)_2(ClO_4)_2]^+$ (HL = 2,6-bis{[(2-hydroxyethyl)(benzyl)amino] methyl}-4-methylphenol) (pK_a = 8.15) [12]. In view of these data, it can be inferred that for $[(H_{-1}\mathbf{L^2})Cu^{II}(\mu\text{-}OH)Cu^{II}(H_2O)]^{2+}$ (**2**c) the titratable proton is from the second Cu(II)-coordinated water molecule, and the formed species is a terminal-hydroxo monocationic species $[(H_{-1}\mathbf{L^2})Cu^{II}(\mu\text{-}OH)Cu^{II}(OH)]^+$ (**2**d). The composition is supported by ESI-MS studies in water/methanol medium where we observed the base peak at m/z = 499.0 amu (calcd. 499.10 amu) matches well with the m/z value of **2**d. The pK_{a3} value of **2** is still lower than the pK_as corresponding to the aquo/terminal hydroxo equilibrium observed for some other structurally related dicopper(II) complexes [40,41,87], which is most likely due to the location of the second Cu(II)-bound water molecule at the equatorial position of a Cu(II) ion in **2**c. This situation probably facilitates the amino or/and the alkylhydroxyl groups in $\mathbf{L^2}$ to act as hydrogen bond donors to the water molecule, similar to the reported previously [39].

By comparison, the pK_a values of **2** are slightly higher than those of **1** in the corresponding deprotonation step, whereas the most attractive case is that further deprotonation of the second Cu(II)-bound water molecule was not observed for **1** in the potentiometric titrations. This different deprotonation behavior implies that the complexation ability of each ligand with Cu(II), the stability and the topology of each complex scaffold may be different, which perhaps exerts impacts on the DNA binding and cleavage of the complexes accordingly.

3.4.2. Complexation equilibria of L^1 and L^2 for Cu(II)

The coordination behavior of $\mathbf{L^1}$ and $\mathbf{L^2}$ was studied in the aqueous methanol solution (CH_3OH/H_2O = 1/1, v/v) containing 0.10 M NaCl in the pH range 3–11 at 298 ± 0.1 K. The equilibrium constants for the complexation reactions of each ligand with Cu(II) were potentiometrically determined and are reported in Table 3. $\mathbf{L^1}$ and $\mathbf{L^2}$ can chelate Cu(II) ion in the aqueous methanol system forming stable mono- and binuclear complexes. Mononuclear species are prevalent in the aqueous solution containing ligand and Cu(II) in 1:1 molar ratio in acidic pH field. Dinuclear species become largely prevalent in the solution starting from slightly acidic pH using a Cu(II)/ligand molar ratio of 2:1, though trace mononuclear species are detected within lower pH range at this molar ratio. This behavior is similar to that reported for the complexes of analogous phenol-based ligands with Cu(II) and other metal ions [19,65]. Fig. 4 illustrates the distribution diagrams of the species for the system ligand/Cu(II) at 1:2 molar ratio as a function of pH. The dinuclear complexes begin to be formed when pH is higher than *ca.* 3.5 for $\mathbf{L^1}$ and *ca.* 3.0 for $\mathbf{L^2}$, and the dinuclear species become the dominant species in the solution when pH is raised to 5.0 for $\mathbf{L^1}$ and to 4.0 for $\mathbf{L^2}$, which suggests $\mathbf{L^2}$ has a stronger ability than $\mathbf{L^1}$ to coordinate Cu(II) ion. The mononuclear $[CuL]^{2+}$ complexes are able to be protonated at lower pH, among which the $[CuL]^{2+}$ species of $\mathbf{L^2}$ shows a higher tendency than that of $\mathbf{L^1}$ to undergo protonation, and $[Cu(H_2L)]^{4+}$ speciation was only observed for $\mathbf{L^2}$ (see Table 3). This different behavior could be reasonably ascribed to far stronger basicity of ethylamino-N atoms of $\mathbf{L^2}$ than that of the pyridyl-N atoms of $\mathbf{L^1}$. The constant values of the deprotonation process for the $[ML]^{2+}$ complexes of both ligands are almost identical (log$K$ = −9.52 and − 9.47 for $\mathbf{L^1}$ and $\mathbf{L^2}$, respectively), suggesting that the acidic proton in $[ML]^{2+}$ is bound to the same donor atom, most plausibly the central phenol-H. For the resultant mononuclear $[Cu(H_{-1}L)]^+$ species the Cu(II) ion is probably complexed by the phenolate-O atom and by N_2O donors of one chelating subunit. The addition of the second Cu(II) ion to $[Cu(H_{-1}L)]^+$ takes place affording the $[Cu_2(H_{-1}L)]^{3+}$ species. The generation process of $[Cu_2(H_{-1}L)]^{3+}$ is very favorable (log$K$ = 10.27 and 11.83 for $\mathbf{L^1}$ and $\mathbf{L^2}$, respectively), implying a similar coordination environment for the two Cu(II) ions, each of which may be stabilized by one ditopic chelating unit and by the phenolate moiety. The molecular topology of $\mathbf{L^1}$ and $\mathbf{L^2}$ facilitates the involvement of the cenral phenolate oxygen in a bridge disposition in the formation of dinuclear complexes as that found in the aforementioned copper(II) complexes derived from the analogous ligands. Additionally, the solution studies highlight a great tendency of the dinuclear $[Cu_2(H_{-1}L)]^{3+}$ species of each ligand to bind a hydroxide generating hydroxylated complexes (7.05 and 6.77 logarithmic units for $\mathbf{L^1}$ and $\mathbf{L^2}$, respectively) over the pH range 5.5–11.0 for $\mathbf{L^1}$ and 5.0–9.0 for $\mathbf{L^2}$, suggesting that the hydroxide anion probably acts as a bridging functionality for saturating the coordination requirement of the two Cu(II) ions in the species. This case is also observed in some copper(II) complexes of analogous ligands bearing aminoalcohol group(s) in aqueous solution [27,42,53]. At pH 7.40, this monohydroxylate complex of each ligand becomes dominant and prevalent in the solution, accounting for about 93% and 66%, respectively, and thereby it can be considered as the active species for the dinuclear complexes **1** and **2** in the interactions with DNA at the pH value. In the case of $\mathbf{L^2}$, a dihydroxylate species $[Cu_2(H_{-1}L)(OH)_2]^+$ having some smaller formation constant (log K = 5.92) was found.

In summary, the aqueous solution studies underline the capability of the two ligands to form stable complexes with Cu(II) ion in aqueous solution. Dinuclear complexes are most the only existing species when a ligand/Cu(II) molar ratio of 1:2 is employed (see Fig. 4). By comparison, the constant values of $\mathbf{L^2}$ for the formation of mono- and di-nuclear complexes are higher than those of $\mathbf{L^1}$, which indicates $\mathbf{L^2}$ has a greater tendency than $\mathbf{L^1}$ to coordinate Cu(II) ion under the same conditions. In particular, the addition of second hydroxide anion to the monohydroxylate dinuclear complex to form dihydroxylate species was observed for $\mathbf{L^2}$ but not for $\mathbf{L^1}$, implying the formation of additional OH^--containing dinuclear species is unfavorable to $\mathbf{L^1}$. As anticipated, both ligands, except for the two same aminoalcohol pendants, feature different chelating arms containing N donors that have distinct nucleophilicity to Cu(II) in aqueous solution. In the case of $\mathbf{L^1}$, the presence of pyridyl groups are capable of decreasing the basicity of the exocyclic nitrogens based on the previous study [79], which may result in a stability decrease of the corresponding complexes. Further, the rigidity of pyridyl moieties may make the molecular topology of $\mathbf{L^1}$ differ from $\mathbf{L^2}$, which may also markedly influence the metal-donor interactions, and thus leads to its poorer performance for stabilization of Cu(II) ion.

On the basis of the characterization data, the above studies and the structurally-related copper(II) complexes reported previously, the two Cu(II) ions in the complexes **1** and **2** are expected to be nested within their respective coordination compartments and are bridged by the endogenous phenoxo O atom of each ligand giving rise to a phenoxido bridge Cu-O-Cu center, respectively. The two aminoalcoholic hydroxyls in each ligand are coordinated to Cu(II) ions while maintaining protonated, similar to lots of copper(II) complexes derived from ligands containing aminoalcohol functionalities [12,27,42,53]. The coordination sphere of each Cu(II) in **1** is completed by an articular tertiary amino-N and a side pendant pyridyl-N donor, whereas in the case of **2**, by an articular tertiary amino-N and a pendant alkyl primary amino-N donor. Exogenous solvent water molecules or/and hydroxy and chloride anions seem to readily occupy the vacant sites of Cu(II) ions in

Table 3
Logarithms of the equilibrium constants for the complexation reactions of **L** with Cu(II) ion determined in 0.10 M NaCl aqueous solution at 298 ± 0.1 K (standard deviations are given in parentheses in the least significant digits).

Reaction	log$K$	
	L^1	L^2
$Cu^{2+} + L = [CuL]^{2+}$	15.52(3)	17.12(3)
$[CuL]^{2+} + H^+ = [CuHL]^{3+}$	4.43(3)	7.15(3)
$[CuHL]^{3+} + H^+ = [Cu_2H_2L]^{3+}$		4.26(3)
$[CuL]^{2+} + H_2O = [Cu(H_{-1}L)]^+ + H_3O^+$	−9.52(2)	−9.47(2)
$[CuL]^{2+} + Cu^{2+} = [Cu_2L]^{4+}$	5.97(3)	6.81(3)
$[Cu(H_{-1}L)]^+ + Cu^{2+} = [Cu_2(H_{-1}L)]^{3+}$	10.27(3)	11.83(3)
$[Cu_2(H_{-1}L)]^+ + OH^- = [Cu_2(H_{-1}L)(OH)]^{2+}$	7.05(3)	6.77(3)
$[Cu_2(H_{-1}L)(OH)]^{2+} + OH^- = [Cu_2(H_{-1}L)(OH)_2]^+$		5.92(3)

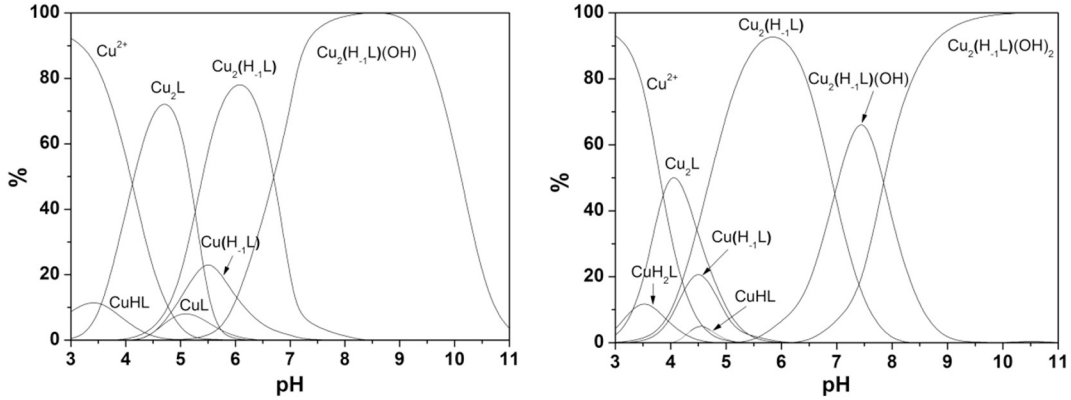

Fig. 4. Species distribution diagrams for $\mathbf{L^1}$/Cu(II) (left) and $\mathbf{L^2}$/Cu(II) (right) as a function of pH in 50% aqueous methanol solution.

each complex, in terminal binding or monoatomic bridging coordination mode, as the structurally analogous copper(II) complexes [14]. It has been known that the coordination number of Cu(II) in the complexes constructed from such type of ligands varies from 4 to 6 [13], among which the 4-coordinate is quite rare in complexes with amino alcohol ligands [90]. In this regard, the five- and six-coordinate spatial arrangements around the two Cu(II) ions within each complex presenting as trigonal bipyramidal (five-coordinate) and octahedral (six-coordinate) geometries are highly expectable (Scheme 2).

3.5. Interactions of *1* and *2* with DNA

Insights into the mode and extent of binding of small molecules such as metal complexes to DNA are important for understanding their DNA cleavage properties. Metal complexes are known to bind to DNA *via* both covalent and non-covalent interactions, and external static electronic interaction, intercalation, and groove binding are three major non-covalent binding modes for metal complexes interacting with DNA [91]. The interactions of the complexes **1** and **2** with DNA were studied by means of absorption and replacement fluorescence techniques with ct-DNA as a substrate.

When **1** and **2** were dissolved respectively in the 50% methanol aqueous HEPES buffer and titrated with ct-DNA at 310 ± 0.2 K, interesting spectral changes in the ligand-based band are observed. As shown in Fig. 5, upon addition of increasing aliquots of ct-DNA to a fixed concentration of each complex (0.11 mM for **1** and 0.18 mM for **2**), a concomitant increase in the absorption intensity at the intraligand absorption bands (239.6 nm for **1** and 241.0 nm for **2**) was observed, similar to a copper(II) complex of a compartmental ligand with two aminohydroxy pendants [92]. Moreover, the spectrum shows slight but discernible blue shifts of *ca.* 4 nm for **1** and *ca.* 2 nm for **2**. The hyperchromicity suggests a non-intercalative or electrostatic binding fashion involved in the interactions of the complexes with DNA because the mode of intercalation in between base pairs of DNA usually results in hypochromism and bathochromism in electronic absorption spectra [92]. The changes in intensity observed for the two complexes on adding ct-DNA follows the trend, **2** > **1**, with the complex **2** of less sterically hindering $\mathbf{L^2}$ affecting slightly prominent. The different extent of blue shifts observed for each complex on DNA binding may also be attributed to the different steric constraints of the substituents in the corresponding ligand, where the sterically hindering pyridyl group in $\mathbf{L^1}$ may render **1** more difficult than **2** to access to DNA. This case further highlights the effects of the substituents on the complex-DNA interactions.

The K_b values for **1** and **2** were determined to be $1.23 \times 10^4\,M^{-1}$ and $6.26 \times 10^4\,M^{-1}$ for ct-DNA, respectively, which are comparable to that of the copper(II) complex derived from a structurally-related ligand [92]. The values of K_b for the corresponding ligands with ct-DNA are $2.02 \times 10^3\,M^{-1}$ and $7.13 \times 10^3\,M^{-1}$. As expected, the K_b value of **2** is higher than that of **1**, most likely due to the lack of steric hindrance in conjunction with the presence of possible hydrogen bonding interactions of the flexible alkylamino chelating arms in $\mathbf{L^2}$ with DNA. Other contributions to the stability of the DNA–complex **2** could be offered by the van der Waals and hydrophobic contacts of cresol ring skeleton with DNA functional groups as complex **1**. The K_b values of the two complexes are significantly lower than those of typical intercalators such as EB ($K_b = 1.4 \times 10^6\,M^{-1}$) [93] and partially intercalating complexes such as heteroleptic $[Cu(tdp)(dipyrido\text{-}[3,2\text{-}d2',3'\text{-}f]\text{-}quinoxaline)]^+$ ($K_b = 9 \times 10^5\,M^{-1}$) [27], indicating the intercalative binding mode appears unlikely for **1** and **2** to interact DNA.

Complementary to the binding mechanistic studies, the competitive binding experiments were carried out on EB-ct-DNA by varying the concentration of each complex in aqueous HEPES buffer (50 mM, pH 7.40) containing 50% methanol to get further insights into the

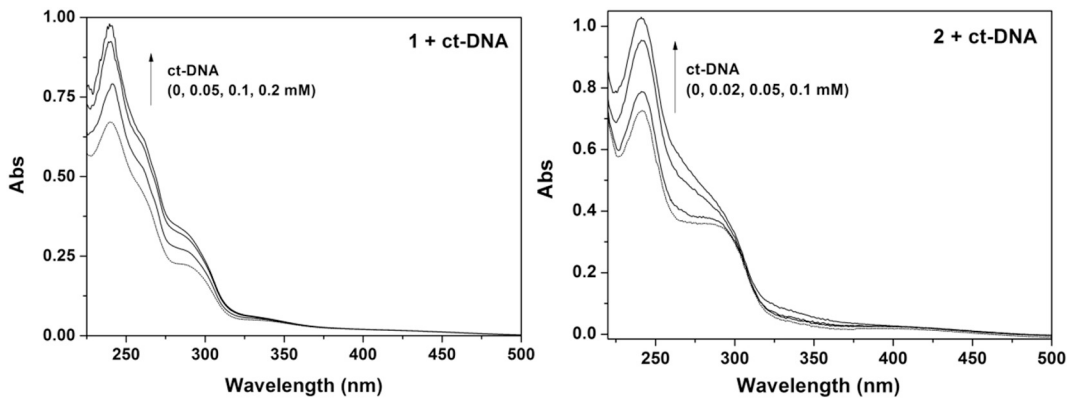

Fig. 5. Absorption spectral traces of **1** and **2** in aqueous 50 mM HEPES/NaCl buffer (pH = 7.40) containing 50% methanol upon addition of ct-DNA.

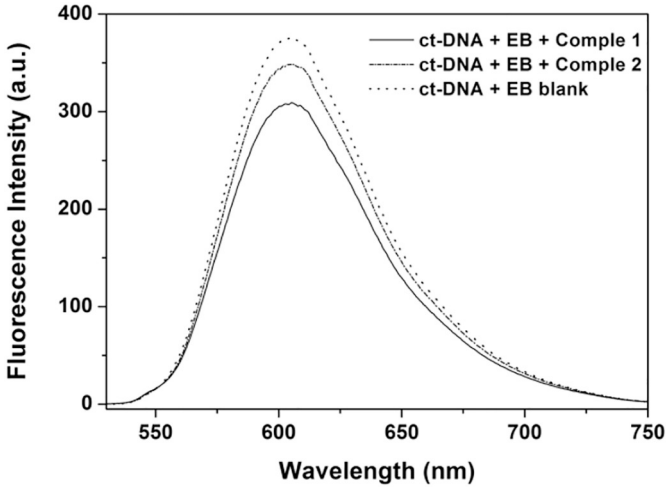

Fig. 6. Emission spectra of ct-DNA-bound EB replaced by the complexes **1** and complex **2** (25 μM) in aqueous 50 mM HEPES/NaCl buffer (pH = 7.40) containing 50% methanol.

complex–DNA interactions at room temperature. As well known, EB is a planar cationic DNA intercalator that can emits intense fluorescence at 605 nm (λ_{em}) upon intercalation between the adjacent base pairs of DNA. The DNA-induced emission of EB would be quenched due to the replacement of the intercalatively bound EB molecule by a second one having stronger binding ability to DNA, and/or the involvement of DNA-mediated electron transfer from the excited EB to an acceptor (*e.g.*, cupric ion, Cu^{2+}) [92]. As shown in Fig. 6, on the addition of 25 μM of the present complexes to the EB-DNA system ([DNA] = [EB] = 25 μM) at 310 ± 0.2 K the emission intensity decreases in 17.9% (**1**) and 7.5% (**2**), respectively, similar to the behaviors for the copper(II) complexes of aminophenol-based ligands [29]. A plausible explanation for the less extend of EB fluorescence quenching induced by **2** than **1** is presumably attributed to the amino chelating arms in $\mathbf{L^2}$ probably being involved in hydrogen bonding interactions with DNA causing the interstrand crosslinking of DNA duplex, which may restrict the release of bound EB [91]. When the cationic **1** and **2** interact with DNA, they probably replace the sodium ions from the compact inner layer or the diffuse outer layer surrounding DNA and then interact with the anionic phosphate residues of DNA. For both complexes, no complete quenching of the DNA-induced emission intensity was observed, indicative of negligible competition between EB and the complexes towards ct-DNA. In addition, the corresponding ligand in **1** and **2** lacks extended π-systems. Thus, it appears that the binding of the complexes to DNA results in some structural changes in DNA, leading to partial release of the intercalatively bound EB. Hence, the observed fluorescence quenching by **1** and **2** is possibly due to the DNA mediated electron transfer resulted from electrostatic interaction or groove binding [92].

It is known that many factors such as size, charge, geometry, chirality, and steric and electronic properties of a small molecule could exert impacts on the binding mode and change extent for DNA [94]. Therefore, extensive studies to evaluate the factors affecting the DNA binding mode are still needed. Taking the above UV–vis and fluorescence spectroscopic results together, a covalent binding to DNA appears unlikely for the complexes **1** and **2**. The cationic property of **1** and **2** may exert a considerable electrostatic attraction to the anionic phosphate backbone of DNA; thus, the electrostatic binding mode is highly possible. Moreover, the major and minor grooves are attractive interacting sites for small molecules, and thus the groove binding mode is also plausible for **1** and **2**. These inferences will be further investigated in the following section, accompanied by the studies of DNA cleavage mechanism.

3.6. DNA cleavage activity of the complexes *1* and *2*

3.6.1. DNA cleavage without addition of ROS scavenger

As potential models of chemical nucleases, we studied the DNA cleaving activity of the complexes **1** and **2** by agarose gel electrophoresis using supercoiled pBR322 DNA as a substrate. The concentration-dependent activity of the complexes was initially investigated under aerobic conditions in the presence of reductant Vc at 310 K during 1 h. As shown in Fig. 7, in the absence or at low concentration (5 μM) of each complex, the plasmid DNA almost remains intact (lanes 1–4), whereas at 10 μM nearly half of Form I DNA is nicked (lane 5) by **1** and **2**. A complete conversion of Form I to Form II occurs at 15 μM (lane 6), and to subsequent linearized DNA (Form III) at *ca* 25 μM is observed for **1** (lane 8). However, for **2** at 15 μM the Form I DNA is completely nicked, and 5% linearized DNA is observed as shown by a continuous band at agarose gel (lane 6). When the concentration of **2** is raised to 25 μM, the lane became very faint, suggesting a majority of DNA has been degraded (lane 8). Further increase in concentration of the complexes results in small undetectable fragments as indicated by a smear on the gel (lane 9). In contrast, Vc and each ligand alone do not induce DNA cleavage under the same other conditions (lanes 2–3). The quantified data for different forms of DNA are listed in Table 4.

The results clearly evidence that both complexes **1** and **2** are capable of nicking and further linearizing the supercoiled DNA at the tested concentrations in the presence of Vc under aerobic conditions. The cleavage activity of **2** is higher than that of **1**, an order in accordance to the DNA binding ability (K_b) of the complexes discussed above, which implicates that the catalytic cleavage activity of the complexes is closely correlated with the DNA-complex binding. In the molecule of **2**, the two primary amino substituents may facilitate the formation of hydrogen-bonding between **2** with DNA as discussed above, which favors **2** geometrically and spatially closer to DNA and more intimate contact in DNA strands compared with **1**, and accordingly results in higher DNA binding. They may also provide hydrogen-bonding sites for the positioning of substrates, similar to a dinuclear Fe(III/II) analogue [15]. However, the complex **1** assembled by the ligand with more bulky and sterically hindered groups may be comparatively difficult to approach DNA, and therefore is unfavorable to DNA cleavage.

The cationic OH^--bridged dicopper(II) complexes of $\mathbf{L^1}$ and $\mathbf{L^2}$ have been shown to be the dominant species in aqueous solution at pH 7.40;

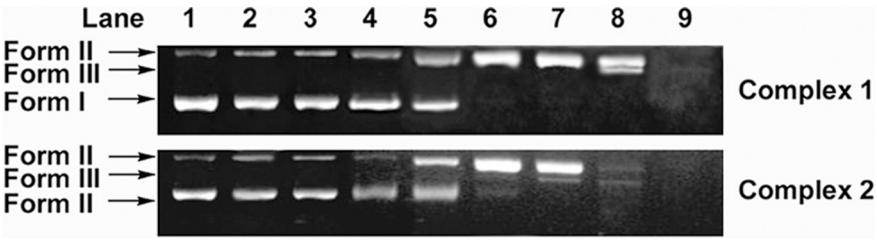

Fig. 7. The cleavage patterns of the agarose gel electrophoresis for pBR322 plasmid DNA (100 ng·μL^{-1}) by the complexes **1** and **2** in 50 mM HEPES buffer (pH 7.40, 25 mM NaCl) at 310 K after 1 h incubation under aerobic conditions.

Table 4
Cleavage efficiency of the complexes **1** and **2** towards pBR322 plasmid DNA at different concentrations (see Fig. 7). The values for each assay are the mean of three independent results obtained under the same conditions.

Complex	Concentration (μM)	Form of DNA (%)		
		I	II	III
DNA control	0	88	12	0
DNA + Vc	0	85	15	0
L[1]	25	88	12	0
Complex **1**	5	73	27	0
	10	61	39	0
	15	2	98	0
	20	0	100	0
	25	0	65	35
L[2]	25	89	11	0
Complex **2**	5	67	33	0
	10	53	47	0
	15	0	95	5
	20	0	85	15
	25	0	52	48

in this case, the observed cleavage activity should arise from their properties. So, it is reasonable to assume that the electrostatic interactions between the cationic complexes and the anionic polynucleotide of DNA may contribute to the binding and consequently the cleavage events. To verify this possibility, assays were performed with increasing concentrations of $LiClO_4$ as a substitute for NaCl to modulate the ionic strength of the reaction media at a fixed concentration of each complex (20 μM) in HEPES buffer (50 mM, pH 7.40). We observed that on increasing the $LiClO_4$ concentrations (25 mM to 100 mM) the DNA cleavage activity of each complex gradually decreased (Fig. S14), similar to the results found in other studies [21]. The cleavage activity of **1** and **2** is almost completely inhibited when the concentration of $LiClO_4$ is raised to 100 mM. These results suggest that Li^+ ions in higher concentrations can compete with the cationic dicopper(II) species to electrostatically interact with the anionic backbone of DNA, which blocks the interaction between the complexes and DNA, and consequently prevents the cleavage.

These results, however, do not rule out groove binding of the complexes with DNA. Thus, assays in the presence of DNA minor groove binder (DAPI) [95] and major groove binder (Methyl Green) [96] were performed (Fig. 8). The plasmid DNA was incubated with the groove binders for 30 min prior to the addition of the present complexes and Vc, and the cleavage reactions were conducted under aerobic conditions at 310 K for 1 h. The agarose gel electrophoresis patterns for the cleavage display that neither DAPI nor methyl green diminishes the DNA cleavage promoted by **1** and **2** (Fig. 8), thereby ruling out the possibility of groove binding mode for the complexes. In these circumstances, **1** and **2** are most likely to interact directly with exterior anionic phosphates of DNA *via* electrostatic attraction, and to cleave the plasmid DNA with the production of diffusible species, like ROS, a main pathway of oxidative mechanism of DNA cleavage [26].

3.6.2. DNA cleavage activity——Hydrolytic versus oxidative cleavage

The topic of hydrolytic and oxidative artificial nucleases has been reviewed several times in the past few years [26,28,30,35]. Due to the

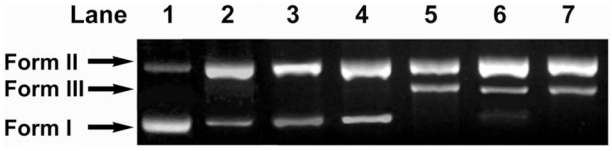

Fig. 8. Agarose gel electrophoresis patterns for the cleavage of pBR322 plasmid DNA (100 ng·μL^{-1}) by **1** (20 μM) and **2** (15 μM) in the presence of DNA groove binding agents in HEPES buffer after 1 h incubation at 310 K.

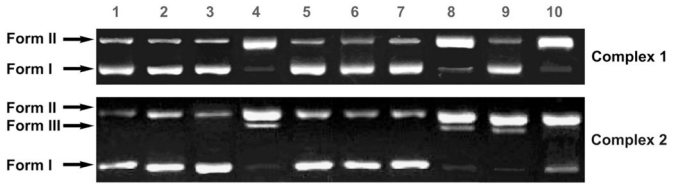

Fig. 9. Cleavage patterns of the agarose gel electrophoresis of supercoiled pBR322 DNA (100 ng·μL^{-1}) treated by **1** (20 μM) and **2** (15 μM) in the presence or absence of ROS scavagers in HEPES buffer after 1 h incubation at 310 K.

irreversibility of the oxidative cleavage, the oxidative cleavers are proposed to be promising candidates for future chemotherapeutics and therefore are of high interest. To examine the mechanism of DNA cleavage promoted by **1** and **2**, the cleavage reactions were initially performed in the absence of Vc activation under the same other conditions as above concentration-dependent experiments. As shown in Fig. 9 (lane 2), the complexes alone exhibit negligible cleavage activity, which suggests an oxidative rather than a hydrolytic mechanism involved in the cleavage promoted by **1** and **2**.

In an oxidative cleavage process, it has been established that molecular oxygen is an essential coreactant involved in the reaction with Cu^{II} to produce a variety of ROS including hydroxyl radicals (OH·), singlet oxygen ($^1O_2$), superoxide anion radical $O_2\cdot^-$), hydrogen peroxide and non-diffusible copper-oxene species [26]. A reductant (Vc or thiol) is normally required to initiate and maintain the radical reaction [51]. The uniqueness of Vc as a reductant in the DNA cleavage reaction may depend on its ability to generate hydrogen peroxide in the presence of dioxygen and metal ions [97]. To assess the role of molecular oxygen in mediating DNA cleavage promoted by **1** and **2**, independent reactions under anaerobic conditions (under dinitrogen gas) were carried out in the presence of Vc. The experimental results given in Fig. 9 (lane 3) evidence that the cleaving reactivities of **1** and **2** are completely suppressed under anaerobic conditions, which underlines the positive effect of the presence of molecular oxygen in the DNA cleavage mediated by **1** and **2**.

In this case, further experiments were conducted to identify ROS possibly involved in the cleavage by adding standard hydroxyl radical scavengers (DMSO, KI and urea), a superoxide anion scavenger (SOD), a singlet oxygen quencher (NaN_3), and hydrogen peroxide scavenger (catalase) prior to addition of each complex and Vc under aerobic conditions. As shown in Fig. 9 (lanes 5–8), compared to the reference without any scavengers (lane 4), the DNA cleavage activities of **1** and **2** were significantly inhibited by DMSO (lane 5), KI (lane 6) and urea (lane 7), but SOD (lane 8), which suggests the involvement of hydroxyl radical intermediates but superoxide anion in the DNA scission. Catalase was also observed to inhibit the cleavage process of the two complexes (lane 9), which is indicative that hydrogen peroxide is necessary in the cleavage. Interestingly, the addition of NaN_3 did not appreciably inhibit the action of **1** (lane 10), ruling out the possible participation of singlet oxygen in its cleavage. However, for complex **2**, the situation is less straightforward; the Form I DNA was completely nicked to Form II while further conversion to Form III DNA was not detected, which suggests the cleavage promoted by **2** was slightly inhibited by singlet oxygen and this kind of ROS is involved in the cleavage reaction.

From these results, it seems reasonable to conclude that the DNA cleavage promoted by **1** and **2** in the presence of Vc under aerobic conditions is an oxidative cleavage process, in which the hydroxyl radical and the hydrogen peroxide generated *in situ* are the active species responsible for the cleavage reactions. For **2**, additional singlet oxygen appears to partially participate in the cleavage, but the DNA-bound ROS (*e.g.* non-diffusible copper-oxene species) as proposed by Sigman et al. [98] for $[Cu(ortho\text{-}phenanthroline)_2]^{2+}$ could not be excluded for the two complexes. As discussed above, the structural modifications of a

ligand molecule are capable of remarkably influencing DNA cleavage activity of the resulting complexes [16,50], and the DNA cleavage efficiency is closely related to the affinity of the complexes to DNA [16]. For the present complexes, the two comparatively bulky methylpyridyl groups on the chelating arms of $\mathbf{L^1}$ were substituted by two ethylamino groups, affording more flexible $\mathbf{L^2}$ with diminished steric encumbrance. The pyridyl groups of $\mathbf{L^1}$ and the amino groups of $\mathbf{L^2}$ both provide N donors with different basicity. Prominently, the two flexible ethylamino chelating arms in $\mathbf{L^2}$ may be susceptible of being involved in hydrogen bonding interactions with DNA, facilitating more stronger binding of **2** with DNA and accordingly affording higher DNA cleavage efficiency, which is almost in agreement with the observations found in the exemplified complexes bearing alkylamino and/or alkylhydroxyl groups. Therefore, it is reasonable to infer that the differences between the introduced substituents of $\mathbf{L^1}$ and $\mathbf{L^2}$ in electronic and steric properties lead to their different capability for Cu(II) complexation, and accordingly the geometry and stability of the resulting complexes, which eventually results in the differences in DNA binding, and DNA cleavage mechanism as well as activity of the complexes in aqueous solution.

4. Conclusion

Two dinuclear copper(II) complexes (**1** and **2**) of phenol-based "end-off" bicompartmental ligands, 2,6-bis{[(2-pyridylmethyl)(2-hydroxyethyl)amino]methyl}-4-methylphenol ($\mathbf{L^1}$) and 2,6-bis{[(2-aminoethyl)(2-hydroxyethyl)amino]methyl}-4-methylphenol ($\mathbf{L^2}$), were prepared and evaluated as potential structural and functional models for the active sites in metallonucleases. Each ligand features a central cresol moiety and two alkylalcohol chelating arms whereas differs in the other arms, *viz.*, two rigid 2-methylpyridyl substituents in $\mathbf{L^1}$ and two flexible 2-ethylamino ones in $\mathbf{L^2}$. The results obtained in ESI-MS, pH potentiometric titrations and spectroscopic analysis show the ligands are inclined to generate dinuclear copper(II) complexes in the case of Cu(II) in excess over the pH range 3–11, and the OH^--bridged cationic dicopper(II) species are the dominant species in aqueous solution at pH 7.40, accounting for *ca.* 93% and 66% respectively. Monitoring of the ESI-MS and UV/Vis spectra of **1** and **2** indicates that the two complexes are stable in aqueous methanol solution for at least 24 h. Both **1** and **2** can bind to ct-DNA through electrostatic attractions with the intrinsic binding constant of **2** ($K_b = 8.96 \times 10^4\,M^{-1}$) being about 5 folds higher than that of **1** ($K_b = 2.23 \times 10^4\,M^{-1}$). They are able to cleave plasmid DNA at submolar concentrations in the presence of Vc under aerobic conditions, displaying a reactivity order of **2** > **1**. Hydroxyl radical and hydrogen peroxide are tested to be active species responsible for the cleavage reactions, interestingly for complex **2** additional singlet oxygen also appears involved in the cleavage. Such pronounced differences between **1** and **2** in DNA binding and cleavage are presumably attributed to the different substituents on the chelating arms of the corresponding ligands. Less steric hindrance of the flexible ethylamino groups in $\mathbf{L^2}$ than the rigid methylpyridyl ones in $\mathbf{L^1}$, together with the additional hydrogen bonding interactions offered by the ethylaminos of **2** with DNA, may facilitate **2** more approach DNA surface and more intimate contact in DNA strands compared with **1**, and hence result in greater DNA cleavage reactivity of **2** than **1**. Moreover, the electron effects of the substituents on the chelating arms, namely, electron withdrawing methylpyridyl groups in $\mathbf{L^1}$ *versus* electron donating ethylamino ones in $\mathbf{L^2}$, may also induce subtle impacts on the properties of the corresponding complexes relevant to DNA cleavage.

The study presented here illustrates the effect of ligand modifications on the DNA binding ability and cleavage catalysis of the resulting complexes. The possible correlations of the electronic and steric properties of the substituents on the pendent arms of the ligands with DNA binding and cleavage of the resulting dicopper(II) complexes were tentatively proposed, even if it's clear that these effects do not control solely the reactivity. The rational design of suitable biomimetic catalytic systems capsable of mimicking the functional properties of metallonucleases continues to be a challenge. The information gained from this study may contribute to expand the comprehension of the structure-function relationship of copper(II)-based model systems showing nuclease-like activity, and may contribute to the development of more efficient catalysts in the future. Still, a deeper knowledge of the factors affecting the reactivity of these dinuclear copper(II) complexes is desirable.

Acknowledgements

We are grateful for the financial support by the National Natural Science Foundation of China (grant No 21775136 and No 21771158), and the Natural Science Foundation of the Higher Education Institutions of Jiangsu Province (grant No. 17KJB150039).

Appendix A. Supplementary data

Supplementary data to this article can be found online at https://doi.org/10.1016/j.jinorgbio.2018.12.014.

References

[1] P.E. Vigato, S. Tamburini, Coord. Chem. Rev. 252 (2008) 1871–1995.
[2] J. Váňa, J. Hanusek, M. Sedlák, Dalton Trans. 47 (2018) 1378–1382.
[3] C. Gerdemann, C. Eicken, B. Krebs, Acc. Chem. Res. 35 (2002) 183–191.
[4] G. Schenk, N. Mitić, G.R. Hanson, P. Comba, Coord. Chem. Rev. 257 (2013) 473–482.
[5] K.D. Karlin, Z. Tyeklar, Bioinorganic Chemistry of Copper, Chapman & Hill, New York, 1993.
[6] R. Krämer, Coord. Chem. Rev. 182 (1999) 243–261.
[7] G. Ambrosi, M. Formica, V. Fusi, L. Giorgi, M. Micheloni, Coord. Chem. Rev. 252 (2008) 1121–1152.
[8] J.R. Gahan, S.J. Smith, A. Neves, G. Schenk, Eur. J. Inorg. Chem. 19 (2009) 2745–2758.
[9] P.A. Vigato, V. Peruzzo, S. Tamburini, Coord. Chem. Rev. 256 (2012) 953–1114.
[10] D. Desbouis, I.P. Troitsky, M.J. Belousoff, L. Spiccia, B. Graham, Coord. Chem. Rev. 256 (2012) 897–937.
[11] G.Q. Feng, D. Natale, R. Prabaharan, J.C. Mareque-Rivas, N.H. Williams, Angew. Chem. Int. Ed. 45 (2006) 7056–7059.
[12] I. Majumder, P. Chakraborty, S. Das, H. Kara, S.K. Chattopadhyay, E. Zangrando, D. Das, RSC Adv. 5 (2015) 51290–51301.
[13] S.S. Massoud, C.C. Ledet, T. Junk, S. Bosch, P. Comba, R. Herchel, J. Hošek, Z. Trávníček, R.C. Fischer, F.A. Mautner, Dalton Trans. 45 (2016) 12933–12950.
[14] R. Sanyal, S. Ketkov, S. Purkait, F.A. Mautner, G. Zhigulin, D. Das, New J. Chem. 41 (2017) 8586–8597.
[15] P. Comba, L.R. Gahan, V. Mereacre, G.R. Hanson, A.K. Powell, G. Schenk, M. Zajaczkowski-Fischer, Inorg. Chem. 51 (2012) 12195–12209.
[16] L.J. Daumann, G. Schenk, D.L. Ollis, L.R. Gahan, Dalton Trans. 43 (2014) 910–928.
[17] P.V. Bernhardt, S. Bosch, P. Comba, L.R. Gahan, G.R. Hanson, V. Mereacre, C.J. Noble, A.K. Powell, G. Schenk, H. Wadepohl, Inorg. Chem. 54 (2015) 7249–7263.
[18] J.J. Brown, L.R. Gahan, A. Schöffler, E.H. Krenske, G. Schenk, J. Inorg. Biochem. 162 (2016) 356–365.
[19] N. Ceccanti, M. Formica, V. Fusi, L. Giorgi, M. Micheloni, R. Pardini, R. Pontellini, M.R. Tinè, Inorg. Chim. Acta 321 (2001) 153–161.
[20] F. Michel, S. Torelli, F. Thomas, C. Duboc, C. Philouze, C. Belle, S. Hamman, E. Saint-Aman, J.-L. Pierre, Angew. Chem. Int. Ed. 44 (2005) 438–441.
[21] T.P. Camargo, F.F. Maia, C. Chaves, B. de Souza, A.J. Bortoluzzi, N. Castilho, T. Bortolotto, H. Terenzi, E.E. Castellano, W. Haase, Z. Tomkowicz, R.A. Peralta, A. Neves, J. Inorg. Biochem. 146 (2015) 77–88.
[22] R.E. Mirams, S.J. Smith, K.S. Hadler, D.L. Ollis, G. Schenk, L.R. Gahan, J. Biol. Inorg. Chem. 13 (2008) 1065–1072.
[23] A. Banerjee, R. Singh, E. Colacio, K.K. Rajak, Eur. J. Inorg. Chem. (2009) 277–284.
[24] T. McGivern, S. Afsharpour, C.J. Marmion, Inorg. Chim. Acta 472 (2018) 12–39.
[25] D.E. Wilcox, Chem. Rev. 96 (1996) 2435–2458.
[26] Q. Jiang, N. Xiao, P.F. Shi, Y.G. Zhu, Z.J. Guo, Coord. Chem. Rev. 251 (2007) 1951–1972.
[27] V. Rajendiran, R. Karthik, M. Palaniandavar, H.S. Evans, V.S. Periasamy, M.A. Akbarsha, B.S. Srinag, H. Krishnamurthy, Inorg. Chem. 46 (2007) 8208–8221.
[28] F. Mancin, P. Scrimin, P. Tecilla, Chem. Commun. 48 (2012) 5545–5559.
[29] R.F. Brissos, E. Torrents, F.M. dos Santos Mello, W.C. Pires, E. de Paula Silveira-Lacerda, A.B. Caballero, A. Caubet, C. Massera, O. Roubeau, S.J. Teat, P. Gamez, Metallomics 6 (2014) 1853–1868.
[30] Z. Yu, J.A. Cowan, Curr. Opin. Chem. Biol. 43 (2018) 37–42.
[31] D. Serre, S. Erbek, N. Berthet, X. Ronot, V. Martel-Frachet, F. Thomas, J. Inorg. Biochem. 179 (2018) 121–134.
[32] C.M. Agbale, M.H. Cardoso, I.K. Galyuon, O.L. Franco, Metallomics 8 (2016) 1159–1169.
[33] D.S. Sigman, A. Mazumder, D.M. Perrin, Chem. Rev. 93 (1993) 2295–2316.

[34] L. Milne, Y. Xu, D.M. Perrin, D.S. Sigman, Proc. Natl. Acad. Sci. U.S.A. 97 (2000) 3136–3141.
[35] C. Santini, M. Pellei, V. Gandin, M. Porchia, F. Tisato, C. Marzano, Chem. Rev. 114 (2014) 815–862.
[36] M. Wehbe, A.W.Y. Leung, M.J. Abrams, C. Orvig, M.B. Bally, Dalton Trans. 46 (2017) 10758–10773.
[37] R.A. Peralta, A.J. Bortoluzzi, B. de Souza, R. Jovito, F.R. Xavier, R.A.A. Couto, A. Casellato, F. Nome, A. Dick, L.R. Gahan, G. Schenk, G.R. Hanson, F.C.S. de Paula, E.C. Pereira-Maia, S. de P. Machado, P.C. Severino, C. Pich, T. Bortolotto, H. Terenzi, E.E. Castellano, A. Neves, M.J. Riley, Inorg. Chem. 49 (2010) 11421–11438.
[38] H. Sakiyama, Y. Igarashi, Y. Nakayama, M.J. Hossain, K. Unoura, Y. Nishida, Inorg. Chim. Acta 351 (2003) 256–260.
[39] M. Wall, B. Linkletter, D. Williams, A.M. Lebuis, R.C. Hynes, J. Chin, J. Am. Chem. Soc. 121 (1999) 4710–4711.
[40] R.E.H.M.B. Osório, R.A. Peralta, A.J. Bortoluzzi, V.R. de Almeida, B. Szpoganicz, F.L. Fischer, H. Terenzi, A.S. Mangrich, K.M. Mantovani, D.E.C. Ferreira, W.R. Rocha, W. Haase, Z. Tomkowicz, A. dos Anjos, A. Neves, Inorg. Chem. 51 (2012) 1569–1589.
[41] C. Belle, C. Beguin, I. Gautier-Luneau, S. Hamman, C. Philouze, J.L. Pierre, F. Thomas, S. Torelli, E. Saint-Aman, M. Bonin, Inorg. Chem. 41 (2002) 479–491.
[42] M.J. Young, D. Wahnon, R.C. Hynes, J. Chin, J. Am. Chem. Soc. 117 (1995) 9441–9447.
[43] E. Kövári, R. Krämer, J. Am. Chem. Soc. 118 (1996) 12704–12709.
[44] M. Forconi, N.H. Williams, Angew. Chem. Int. Ed. 41 (2002) 849–852.
[45] M. Livieri, F. Mancin, U. Tonellato, J. Chin, Chem. Commun. (2004) 2862–2863.
[46] J. Chin, S. Chung, D.H. Kim, J. Am. Chem. Soc. 124 (2002) 10948–10949.
[47] J.C. Mareque-Rivas, R.T.M. de Rosales, S. Parsons, Chem. Commun. (2004) 610–611.
[48] X. Sheng, X.M. Lu, Y.T. Chen, G.Y. Lu, J.J. Zhang, Y. Shao, F. Liu, Q. Xu, Chem. Eur. J. 13 (2007) 9703–9712.
[49] X.P. Zhang, X.P. Liu, D.L. Phillips, C.Y. Zhao, Dalton Trans. 45 (2016) 1593–1603.
[50] A.A. Janitra, S. Tjakraatmadja, C. Lüdtke, N. Kulak, Inorg. Chim. Acta 452 (2016) 159–169.
[51] S. Claudia, M. Fabrizio, G. Maddalena, P. Manlio, T. Paolo, T. Umberto, Inorg. Chem. 44 (2005) 2310–2317.
[52] A.J. Dyckman, J. Med. Chem. 60 (2017) 5267–5289.
[53] V. Rajendiran, M. Palaniandavar, P. Swaminathan, L. Uma, Inorg. Chem. 46 (2007) 10446–10448.
[54] L.J. Daumann, K.E. Dalle, G. Schenk, R.P. McGeary, P.V. Bernhardt, D.L. Ollis, L.R. Gahan, Dalton Trans. 41 (2012) 1695–1708.
[55] J.W. Chen, X.Y. Wang, Y.G. Zhu, J. Lin, X.L. Yang, Y.Z. Li, Y. Lu, Z.J. Guo, Inorg. Chem. 44 (2005) 3422–3430.
[56] J.W. Chen, X.Y. Wang, Y. Shao, J.H. Zhu, Y.G. Zhu, Y.Z. Li, Q. Xu, Z.J. Guo, Inorg. Chem. 46 (2007) 3306–3312.
[57] W.L.E. Armarego, D.D. Perrin, Purification of Laboratory Chemicals, 4th ed., Butterworth-Heinemann, Wodburn, MA, 2000.
[58] ISOPRO, Mike Senko, 243 Buena Vista Ave. #502, Sunnyvale, CA 94086, USA, http://members, (1998) aol.com/msmssoft.
[59] H.P. Berends, D.W. Stephen, Inorg. Chem. 26 (1987) 749–754.
[60] R.A. Peralta, A. Neves, A.J. Bortoluzzi, A. dos Anjos, F.R. Xavier, B. Szpoganicz, H. Terenzi, M.C.B. de Oliveira, E. Castellano, G.R. Friedermann, A.S. Mangrich, M.A. Novak, J. Inorg. Biochem. 100 (2006) 992–1004.
[61] A.E. Martell, R.J. Motekaitis, P.S. Mahe (Ed.), Determination and Use of Stability Constants, 2nd edition, John Wiley & Sons, New York, 1992.
[62] J. Marmur, J. Mol. Biol. 3 (1961) 208–214.
[63] M.E. Reichmann, S.A. Rice, C.A. Thomas, P. Doty, J. Am. Chem. Soc. 76 (1954) 3047–3053.
[64] A. Wolfe, G.H. Shimer, T. Meehan, Biochemistry 26 (1987) 6392–6396.
[65] N.A. Rey, A. Neves, P.P. Silva, F.C.S. Paula, J.N. Silveira, F.V. Botelho, L.Q. Vieira, C.T. Pich, H. Terenzi, E.C. Pereira-Maia, J. Inorg. Biochem. 103 (2009) 1323–1330.
[66] Y. Jin, J.A. Cowan, J. Am. Chem. Soc. 127 (2005) 8408–8415.
[67] H. Ahsan, S.M. Hadi, Cancer Lett. 124 (1998) 23–30.
[68] A. Sreedhara, J.D. Freed, J.A. Cowan, J. Am. Chem. Soc. 122 (2000) 8814–8824.
[69] B. Halliwell, J.M.C. Gutteridge, Superoxide Dismutase 3 (1985) 45–82.
[70] K.S. Bharathi, A.K. Rahiman, K. Rajesh, S. Sreedaran, P.G. Aravindan, D. Velmurugan, V. Narayanan, Polyhedron 25 (2006) 2859–2868.
[71] L.J.H. Borges, É.S. Bull, C. Fernandes, A. Horn Jr., N.F. Azeredo, J.A.L.C. Resende, W.R. Freitas, E.C.Q. Carvalho, L.S. Lemos, H. Jerdy, M.M. Kanashiro, Eur. J. Med. Chem. 123 (2016) 128–140.
[72] D. Saravanakumar, N. Sengottuvelan, G. Priyadarshni, M. Kandaswamy, H. Ōkawa, Polyhedron 23 (2004) 665–672.
[73] S. Rodríguez-Hermida, C. Wende, A.B. Lago, R. Carballo, N. Kulak, E.M. Vázquez-López, Eur. J. Inorg. Chem. (2013) 5843–5853.
[74] S.K. Mandal, K. Nag, J. Chem, J. Chem. Soc. Dalton Trans. (1984) 2141–2149.
[75] K. Nakamoto, Infrared Spectra and Raman Spectra of Inorganic and Coordination Compounds, John Wiley & Sons, New York, 1997.
[76] E. Berti, A. Caneschi, C. Daiguebonne, P. Dapporto, M. Formica, V. Fusi, L. Giorgi, A. Guerri, M. Micheloni, P. Paoli, R. Pontellini, P. Rossi, Inorg. Chem. 42 (42) (2003) 348–357.
[77] K.S. Banu, T. Chattopadhyay, A. Banerjee, S. Bhattacharya, E. Suresh, M. Nethaji, E. Zangrando, D. Das, Inorg. Chem. 47 (2008) 7083–7093.
[78] S. Anbu, M. Kandaswamy, P. Suthakaran, V. Murugan, B. Varghese, J. Inorg. Biochem. 103 (2009) 401–410.
[79] S. Laine, C.S. Bonnet, F.K. Kálmán, Z. Garda, A. Pallier, F. Caillé, F. Suzenet, G. Tircsó, É. Tóth, New J. Chem. 42 (2018) 8012–8020.
[80] M. Jarenmark, E. Csapó, J. Singh, Simone Wöckel, E. Farkas, F. Meyer, M. Haukka, E. Nordlander, Dalton Trans. 39 (2010) 8183–8194.
[81] W.M. Haynes, CRC Handbook of Chemistry and Physics, 92nd edition, CRC Press, Taylor and Francis, Boca Raton, FL, 2011.
[82] A.V. Rayer, K.Z. Sumon, L. Jaffari, A. Henni, J. Chem. Eng. Data 59 (2014) 3805–3813.
[83] E.S. Hamborg, G.F. Versteeg, J. Chem. Eng. Data 54 (2009) 1318–1328.
[84] M. Zhao, H.L. Wang, L. Zhang, C.Y. Zhao, L.N. Ji, Z.W. Mao, Chem. Commun. 47 (2011) 7344–7346.
[85] V.R. de Almeida, F.R. Xavier, Renata E.H.M.B. Osório, L.M. Bessa, E.L. Schilling, T.G. Costa, T. Bortolotto, A. Cavalett, Frederico A.V. Castro, F. Vilhena, O.C. Alves, H. Terenzi, Elis C.A. Eleutherio, M.D. Pereira, W. Haase, Z. Tomkowicz, B. Szpoganicz, A.J. Bortoluzzi, A. Neves, Dalton Trans. 42 (2013) 7059–7073.
[86] A. Thibon-Pourret, F. Gennarini, R. David, J.A. Isaac, I. Lopez, G. Gellon, F. Molton, L. Wojcik, C. Philouze, D. Flot, Y.L. Mest, M. Réglier, N.L. Poul, H. Jamet, C. Belle, Inorg. Chem. 57 (2018) 12364–12375.
[87] S. Torelli, C. Belle, I. Gautier-Luneau, J.L. Pierre, E. Saint-Aman, J.M. Latour, L.L. Pape, D. Luneau, Inorg. Chem. 39 (2000) 3526–3536.
[88] M. Lanznaster, A. Neves, A.J. Bortoluzzi, V.E. Aires, B. Szpoganicz, H. Terenzi, P.C. Severino, J.M. Fuller, S.C. Drew, L.R. Gahan, G.R. Hanson, M.J. Riley, G. Schenk, J. Biol. Inorg. Chem. 10 (2005) 319–332.
[89] C. Fernandes, A. Neves, A.J. Bortoluzzi, A.S. Mangrich, E. Rentschler, B. Szpoganicz, E. Schwingel, Inorg. Chim. Acta 320 (2001) 12–21.
[90] P. Seppälä, R. Sillanpää, A. Lehtonen, Coord. Chem. Rev. 347 (2017) 98–114.
[91] A. Raja, V. Rajendiran, P.U. Maheswari, R. Balamurugan, C.A. Kilner, M.A. Halcrow, M. Palaniandavar, J. Inorg. Biochem. 99 (2005) 1717–1732.
[92] D. Mandal, M. Chauhan, F. Arjmand, G. Aromí, D. Ray, Dalton Trans. (2009) 9183–9191.
[93] M. Baldini, M. Belicchi-Ferrari, F. Bisceglie, P.P. Dall'Aglio, G. Pelosi, S. Pinelli, P. Tarasconi, Inorg. Chem. 43 (2004) 7170–7179.
[94] J.K. Barton, I. Bertini, H.B. Gray, S.J. Lippard, J.S. Valentine (Eds.), Bioinorganic Chemistry, University Press, Mill Valley, CA, 1994, pp. 455–503.
[95] E. Trotta, N. Del Grosso, M. Erba, M. Paci, Biochemistry 39 (2000) 6799–6808.
[96] P. Wittung, P. Nielsen, B. Norden, J. Am. Chem. Soc. 118 (1996) 7049–7054.
[97] S.H. Chiou, N. Ohtsu, K.G. Bensch, D. Karlin, J. Zubieta (Eds.), Biological and Inorganic Copper Chemistry, Adenine Press, New York, 1985, pp. 119–123.
[98] D.S. Sigman, Biochemistry 29 (1990) 9097–9105.